J. Fluid Mech. (1996), vol. 308, pp. 255–288

Computer simulations of polymer chain relaxation via Brownian motion

By P. GRASSIA[1] AND E. J. HINCH[2]

[1]Departamento de Física, Universidad de Chile, Av. Blanco Encalada 2008, Casilla 487-3, Santiago, Chile

[2] Department of Applied Mathematics and Theoretical Physics, The University of Cambridge, Silver Street, Cambridge CB3 9EW, UK

(Received 6 December 1994 and in revised form 15 September 1995)

Numerical simulations are employed to study the Brownian motion of a bead–rod polymer chain dissolved in a solvent. An investigation is conducted of the relaxation of the stress for an initially straight chain as it begins to coil.

For a numerical time step δt in the simulations, conventional formulae for the stress involve averaging large $\pm O(1/(\delta t)^{1/2})$ contributions over many realizations, in order to yield an $O(1)$ average. An alternative formula for the stress is derived which only contains $O(1)$ contributions, thereby improving the quality of the statistics.

For a chain consisting of n rods in a solvent at temperature $\hat{T}$, the component of the bulk stress along the initial chain direction arising from tensions in the rods at the initial instant is $k\hat{T} \times n(\frac{1}{3}n^2 + n + \frac{2}{3})$. Thus the bead–rod model yields results very different from other polymer models, such as the entropic spring of Flory (1969), which would assign an infinite stress to a fully aligned chain. For rods of length $\hat{l}$ and beads of friction factor $\hat{\zeta}$, the stress decays at first on $O(\hat{\zeta}\hat{l}^2/k\hat{T} \times 1/n^2)$ time scales. On longer time scales, this behaviour gives way to a more gradual stress decay, characterized by an $O(k\hat{T} \times n)$ stress following a simple exponential decay with an $O(k\hat{T}/\hat{\zeta}\hat{l}^2 \times 1/n^2)$ rate. Matching these two limiting regimes, a power law decay in time $\hat{t}$ is found with stress $O(k\hat{T} \times n^2 \times (k\hat{T}\hat{t}/\hat{\zeta}\hat{l}^2)^{-1/2})$. The dominant physical processes occurring in these separate short, long and intermediate time regimes are identified.

1. Simple models of polymer microstructure

In order to obtain realistic constitutive relations describing polymeric solutions, rheologists increasingly realize that it is necessary to incorporate polymer microstructure into constitutive models. The simplest possible microstructural model for a polymeric chain replaces a long chain possessing a multiplicity of monomer units by an elastic dumbbell, consisting of two beads joined by an elastic link (see e.g. Hinch 1977; Bird *et al.* 1987 and Rallison & Hinch 1988).

The force law in the elastic dumbbell might in the simplest case be Hookean, i.e. linear springs. Alternatively we could use a so-called 'entropic spring' with an 'inverse Langevin' force law (Flory 1969), or some other force law with finite extensibility, viz. the well known 'Finitely Extensible Nonlinear Elastic' (FENE) dumbbell (Bird *et al.* 1987; Rallison & Hinch 1988). We may also want to incorporate springs with a non-zero natural length. The Fraenkel spring force law for instance assumes a force with magnitude proportional to the difference between the actual spring length and some natural length (Bird *et al.* 1987).

Clearly we can extend the model beyond a dumbbell, by joining together many beads with elastic links, taking each bead to be subject to random thermal forces (Ermak & McCammon 1978; Fixman 1978*a*; Bird *et al.* 1987). The links may be either Hookean, FENE or Fraenkel springs. When an arbitrary number of beads are joined by Hookean springs we obtain the so-called Rouse model (Rouse 1953; Bird *et al.* 1987) and if hydrodynamic interactions between the beads are incorporated we obtain the Zimm model (Zimm 1956; Bird *et al.* 1987).

This paper will initially focus on bead–spring chains in which the links are Fraenkel rather than Hookean springs, but for which hydrodynamic interactions are ignored. We shall therefore be considering a modification of the Rouse model. By inserting realistic physical parameters into the model, we shall show that the available thermal energy is only sufficient to deform the springs by a small fraction of their natural length, i.e. the springs are stiff. Thus it is appropriate to replace a bead–spring chain by one in which the beads are joined by rigid (i.e. inextensible) links. This is the so-called bead–rod model (Kramers 1946; Kirkwood & Riseman 1956; Hassager 1974; Ermak & McCammon 1978; Fixman 1978*a*; Liu 1989).

This latter model will be used in the bulk of the numerical computations to be presented in the paper. We shall employ a stochastic simulation technique to study the effects of Brownian motion on the model polymer chain. Naive computer simulations of the bead–rod model however lead to erroneous results (Grassia, Hinch & Nitsche 1995). Modifications to the algorithm are necessary (Ermak & McCammon 1978; Fixman 1978*a*) in order for simulations to model correctly the configurational changes of very stiff bead–spring chains. We shall describe these modifications and produce a corrected simulation technique.

The long term aim of studying Brownian motion of polymer chains is to produce suitable constitutive equations for polymer solutions. It may be impractical to incorporate every single feature of the simulations into a constitutive relation. Nonetheless it is hoped that the simulations will elucidate the key features of polymer chain physics which govern constitutive behaviour.

One of the important issues that we aim to address is the following. Given the dynamics of a single link, how does the presence of many links affect the dynamics of the chain as a whole? In other words, how are time scales for the evolution of the chain configuration related to the evolution time scale of a single link? As we shall see, the bead–rod chain model unambiguously addresses this question.

The problem that we shall simulate in this paper is the stress relaxation in the initially straight bead–rod chain. Physically this corresponds to the chain being stretched fully by a very strong flow and then the flow being switched off suddenly. Some of the questions we pose are as follows. Is the stress finite at the initial instant, and if so what is its value? Can we identify distinct regimes of chain evolution and the physics governing each regime?

2. Formulation of the bead–spring model

In this section we shall formulate the equations describing the Brownian motion of polymer chains. Then we shall non-dimensionalize these equations and identify governing dimensionless groups.

We consider a polymer chain dissolved in a viscous solvent at temperature $\hat{T}$. Suppose the bead–spring polymer chain consists of $n+1$ beads and n links. Label the bead positions by $\hat{\boldsymbol{X}}_i$, $0 \leqslant i \leqslant n$. For $1 \leqslant i \leqslant n$, let $\hat{\boldsymbol{D}}_i$ denote $\hat{\boldsymbol{X}}_i - \hat{\boldsymbol{X}}_{i-1}$, the vector joining two beads across a link. We define a link length $\hat{l}_i = (\hat{\boldsymbol{D}}_i \cdot \hat{\boldsymbol{D}}_i)^{1/2}$ and a unit

vector along the link direction $\boldsymbol{d}_i = \hat{\boldsymbol{D}}_i/(\hat{\boldsymbol{D}}_i \cdot \hat{\boldsymbol{D}}_i)^{1/2}$. Throughout the paper we shall employ the notation that '^' denotes a dimensional quantity. Removing the '^' from a symbol gives the dimensionless analogue.

Three types of forces act on the beads: viscous drag, tension forces in the links and random Brownian forces. We consider each in turn.

The viscous drag is assumed to be linear in the bead velocity with a constant of proportionality $\hat{\zeta}$, known as the friction factor. Following Ermak & McCammon (1978) and Fixman (1978*a*) we discard the inertia of the beads. Physically this can be shown to imply that drag forces make a bead 'forget' its initial velocity long before the direction of a link significantly changes. Grassia (1994) has estimated the ratio of this 'memory' time for bead velocity to the time scale for link directional changes, obtaining values 8×10^{-5}–5×10^{-4}. This estimate involves data gathered from several sources (Weast 1971–72; Kaye & Laby 1973; Abe, Jernigan & Flory 1966; Flory 1969).

We shall suppose that the links are Fraenkel springs with a natural length $\hat{l}$ and a spring constant $\hat{K}$. Stretching or compressing the springs will lead to tensions in the links $\hat{\tau}_i^{sp}$ with

$$\hat{\tau}_i^{sp} = \hat{K}(\hat{l}_i - \hat{l}).$$

The energy associated with stretching the links is thus $\frac{1}{2}\hat{K}(\hat{l}_i - \hat{l})^2$. The force on bead $i-1$ due to the tension $\hat{\tau}_i^{sp}$ will be $\hat{\tau}_i^{sp}\boldsymbol{d}_i$ while the force on bead i will be $-\hat{\tau}_i^{sp}\boldsymbol{d}_i$. The net tension force on bead i arises from tensions in both link i and in link $i+1$, and is $\hat{\tau}_{i+1}^{sp}\boldsymbol{d}_{i+1} - \hat{\tau}_i^{sp}\boldsymbol{d}_i$. Note that there is no elastic force associated with changing the link direction $\boldsymbol{d}_i$, only with changing link length $\hat{l}_i$. This implies that the links are freely jointed.

The beads are also subjected to random bombardments from the solvent molecules, giving a fluctuating random force. We write the fluctuating force on bead i at time $\hat{T}$ as $\hat{\boldsymbol{F}}_i^{ra}(\hat{t})$. Note that $\hat{\boldsymbol{F}}_i^{ra}(\hat{t})$ has zero mean. We also make the 'white noise' assumption for the random forcing, i.e. we assume that the random force is uncorrelated between any two different instants of time. A general theorem from statistical mechanics, the fluctuation-dissipation theorem (see e.g. Reif 1965; Ermak & McCammon 1978; Fixman 1978*a*; Grassia *et al.* 1995 and Hinch 1994), relates the mean square value of the fluctuating force to the friction factor

$$\langle \hat{\boldsymbol{F}}_i^{ra}(\hat{t})\hat{\boldsymbol{F}}_j^{ra}(\hat{t}')\rangle = 2k\hat{T}\hat{\zeta}\boldsymbol{I}\delta_{ij}\delta(\hat{t}-\hat{t}').$$

Here $\langle\,\rangle$ denotes the expectation value, k denotes Boltzmann's constant, $\boldsymbol{I}$ is the 3×3 identity tensor, δ_{ij} is the Kronecker delta for beads i and j and $\delta(\hat{t}-\hat{t}')$ is the Dirac delta function at times t and t'. The theorem is merely a mathematical statement that on average the work done by the random forces balances the energy lost to viscous dissipation. For beads of non-zero inertia, this ensures that the average bead kinetic energy remains constant, which is physically necessary since the polymer is in thermal contact with the solvent at temperature $\hat{T}$. However for the present case of vanishing bead inertia, the 'theorem' must be assumed, not proven.

The sum of tension forces, random forces and viscous drag must vanish for negligible bead inertia. Mathematically we have

$$\hat{\zeta}\frac{\mathrm{d}\hat{\boldsymbol{X}}_i}{\mathrm{d}\hat{t}} = \hat{\boldsymbol{F}}_i^{ra}(\hat{t}) + \hat{\tau}_{i+1}^{sp}\boldsymbol{d}_{i+1} - \hat{\tau}_i^{sp}\boldsymbol{d}_i.$$

For more detailed discussions see Ermak & McCammon (1978), Fixman (1978*a*), Grassia *et al.* (1995) and Hinch (1994).

Now we non-dimensionalize the above equations. We let $\boldsymbol{X}_i = \hat{\boldsymbol{X}}_i/\hat{l}$, $\boldsymbol{D}_i = \hat{\boldsymbol{D}}_i/\hat{l}$ and $l_i = \hat{l}_i/\hat{l}$. The unit link director $\boldsymbol{d}_i$ is already dimensionless, and can be expressed as $\boldsymbol{D}_i/(\boldsymbol{D}_i \cdot \boldsymbol{D}_i)^{1/2}$. Observe moreover that $l_i = (\boldsymbol{D}_i \cdot \boldsymbol{D}_i)^{1/2}$.

We define a non-dimensional time t as $t = k\hat{T}\hat{t}/\hat{\zeta}\hat{l}^2$, and in future will use a dot to denote differentiation with respect to dimensionless t rather than dimensional $\hat{t}$. Since $k\hat{T}/\hat{\zeta}$ is a diffusivity (the Stokes–Einstein relation), it is evident that we have chosen to non-dimensionalize $\hat{t}$ according to the diffusion time scale of an individual link. As implied in the discussion of §1, a purpose of this paper is to investigate how this time scale is changed by the existence of n links, with in principle n being a large number.

Dimensionless link tensions τ_i^{sp} are defined as $\tau_i^{sp} = \hat{\tau}_i^{sp}\hat{l}/k\hat{T}$ and dimensionless random forces as $\boldsymbol{F}_i^{ra}(t) = \hat{\boldsymbol{F}}_i^{ra}(\hat{t})\hat{l}/k\hat{T}$. We also define a dimensionless group

$$K = \frac{\hat{K}\hat{l}^2}{k\hat{T}},$$

which is a dimensionless analogue of the spring constant.

The equations governing this bead–spring model are thus

$$\tau_i^{sp} = K(l_i - 1) \qquad \text{(spring force law)},$$

$$\langle \boldsymbol{F}_i^{ra}(t)\boldsymbol{F}_j^{ra}(t')\rangle = 2\boldsymbol{I}\delta_{ij}\delta(t-t') \qquad \text{(fluctuation dissipation theorem)},$$

$$\dot{\boldsymbol{X}}_i = \boldsymbol{F}_i^{ra}(t) + \tau_{i+1}^{sp}\boldsymbol{d}_{i+1} - \tau_i^{sp}\boldsymbol{d}_i. \qquad \text{(equation of motion)}.$$

Note that the dimensionless spring energy is $\frac{1}{2}K(l_i - 1)^2$.

3. Bead–spring numerical algorithm

In order to simulate the above equations numerically we must replace the differential equations by a discrete time-stepping scheme. Numerical schemes abound in the stochastic calculus literature (Kloeden & Platen 1980; Øskendal 1985). For schemes in the context of polymer dynamics refer to Ermak & McCammon (1978), Fixman (1978*a*) and Grassia *et al.* (1995).

In a numerical scheme the first task of any discrete time step is to assign the random forces $\boldsymbol{F}_i^{ra}$. Let us denote the size of the time step by δt. For a chain of $n+1$ beads, we select $n+1$ independent random vectors $\boldsymbol{n}_i$, $0 \leqslant i \leqslant n$, each with independent components uniformly distributed on $[-1, 1]$. Then we assign the random force on bead i, denoted $\boldsymbol{F}_i^{ra}$, to be $(6/\delta t)^{1/2}\boldsymbol{n}_i$. We shall employ the notation that $(\boldsymbol{F}_i^{ra})_I$ is the random force applying on the time step between times $I\,\delta t$ and $(I+1)\,\delta t$.

With the above definition of random forces we find

$$\langle (\boldsymbol{F}_i^{ra})_I (\boldsymbol{F}_j^{ra})_J \rangle = \frac{2\boldsymbol{I}\delta_{ij}\delta_{IJ}}{\delta t},$$

which is the discrete approximation to the fluctuation-dissipation theorem.

The bead motion will be described numerically by a midpoint rule. Subscripted parentheses placed around variables, $()_0$, $()_{1/2}$ and $()_1$, will denote values at the beginning, midpoint and end of a step respectively. For instance, for the first time

step, the midpoint rule can be written

$$(\boldsymbol{X}_i)_{1/2} = (\boldsymbol{X}_i)_0 + \frac{\delta t}{2}\Big((\boldsymbol{F}_i^{ra})_0 + (\tau_{i+1}^{sp})_0(\boldsymbol{d}_{i+1})_0 - (\tau_i^{sp})_0(\boldsymbol{d}_i)_0\Big),$$
$$(\boldsymbol{X}_i)_1 = (\boldsymbol{X}_i)_0 + \delta t\left((\boldsymbol{F}_i^{ra})_0 + (\tau_{i+1}^{sp})_{1/2}(\boldsymbol{d}_{i+1})_{1/2} - (\tau_i^{sp})_{1/2}(\boldsymbol{d}_i)_{1/2}\right).$$

In fact a simple forward time-stepping scheme would have been adequate here (Grassia *et al.* 1995), but the midpoint rule leads to smaller truncation errors in certain quantities, e.g. the energy stored in the elastic links.

4. Bead–spring formula for stress

The previous section gave a numerical scheme which can be used to follow the Brownian evolution of a bead–spring chain. If we want to study the rheology of polymer chains then we need to be able to calculate the bulk stress contribution of the chain, given the configuration and the forces acting. This section describes the formula used for the stress calculation and adapts it to the numerical scheme. Throughout this paper we shall use the term 'stress' to imply 'bulk stress contribution per chain'.

We shall denote stress by $\boldsymbol{\sigma}$. For a polymer chain whose beads are acted on by forces $\boldsymbol{F}_i^{ra}$, with in addition tensions τ_i^{sp} in the links, Kramers' expression for the stress (Bird *et al.* 1987) is

$$\boldsymbol{\sigma} = -\sum_{i=0}^{n}\langle \boldsymbol{X}_i(\boldsymbol{F}_i^{ra} + \tau_{i+1}^{sp}\boldsymbol{d}_{i+1} - \tau_i^{sp}\boldsymbol{d}_i)\rangle \qquad \text{(Kramers' stress formula)}$$
$$= -\sum_{i=0}^{n}\langle \boldsymbol{X}_i\boldsymbol{F}_i^{ra}\rangle + \sum_{i=1}^{n}\langle \tau_i^{sp} l_i \boldsymbol{d}_i\boldsymbol{d}_i\rangle.$$

In the the second line we have used $\boldsymbol{X}_i - \boldsymbol{X}_{i-1} = \boldsymbol{D}_i = l_i\boldsymbol{d}_i$.

The $\langle\,\rangle$ symbols denote an (ensemble) expectation, which corresponds numerically to an average over many realizations of a simulation. For a bead–spring chain in a known configuration the tensions are deterministic. Nonetheless we retain the expectation symbols around $\tau_i^{sp} l_i \boldsymbol{d}_i\boldsymbol{d}_i$, since the configuration is itself random, having been produced by past random forcing.

The Kramers stress formula needs to be adapted and interpreted for numerical work. Especially problematic is that numerically $\boldsymbol{X}_i\boldsymbol{F}_i^{ra}$ is $\pm O(1/(\delta t)^{1/2})$, yet we presumably want to average many such quantities and obtain an $O(1)$ stress. Prohibitively many realizations may be required to obtain good statistics. Note that when we refer to quantities as being '$O(1/(\delta t)^{1/2})$' or '$O(1)$' in the present section, we are of course ignoring factors expressing how the stress depends on the number of links n.

The stress formula as written in the above equation has a random forcing component and a spring tension component. Let us call them $\boldsymbol{\sigma}_{ra}$ and $\boldsymbol{\sigma}_{sp}$ say. Suppose we want to calculate the stress after the first time step. The numerical calculation of $\boldsymbol{\sigma}_{sp}$ is straightforward and is

$$\boldsymbol{\sigma}_{sp} = \sum_{i=1}^{n}\langle (\tau_i^{sp})_1 (l_i)_1 (\boldsymbol{d}_i)_1 (\boldsymbol{d}_i)_1\rangle.$$

The appropriate numerical formula for $\boldsymbol{\sigma}_{ra}$ is less obvious, since the random force on bead i changes discontinuously at the end of the step from $(\boldsymbol{F}_i^{ra})_0$ to $(\boldsymbol{F}_i^{ra})_1$. We

take the mean of these values when calculating $\boldsymbol{\sigma}_{ra}$. However $(\boldsymbol{X}_i)_1$ is independent of $(\boldsymbol{F}_i^{ra})_1$, so that each $-\frac{1}{2}(\boldsymbol{X}_i)_1(\boldsymbol{F}_i^{ra})_1$ can be dropped from the $\boldsymbol{\sigma}_{ra}$ formula, leaving $-\frac{1}{2}(\boldsymbol{X}_i)_1(\boldsymbol{F}_i^{ra})_0$ to be summed over the beads. This is still a $\pm O(1/(\delta t)^{1/2})$ quantity. However now we make the observation that $(\boldsymbol{X}_i)_0$ is independent of $(\boldsymbol{F}_i^{ra})_0$, so that an equally good formula for $\boldsymbol{\sigma}_{ra}$ is

$$\boldsymbol{\sigma}_{ra} = -\sum_{i=0}^{n} \tfrac{1}{2} \langle ((\boldsymbol{X}_i)_1 - (\boldsymbol{X}_i)_0)(\boldsymbol{F}_i^{ra})_0 \rangle .$$

This involves averaging $O(1)$ not $O(1/(\delta t)^{1/2})$ quantities, so should give better statistics.

The seemingly artificial requirement of taking the random force to be the mean of $(\boldsymbol{F}_i^{ra})_0$ and $(\boldsymbol{F}_i^{ra})_1$ is a result of assuming vanishing bead inertia. For non-zero bead inertia, obtaining the correct stress would not rely on correlations between the fluctuating part of the force and the particle displacement, so there would be no numerical ambiguities concerning discontinuous random forcing. For chains of no inertia, the factor $\frac{1}{2}$ in $\boldsymbol{\sigma}_{ra}$ must be included to make the overall stress $\boldsymbol{\sigma}$ agree with that of an inertial chain (in the limit as chain inertia approaches zero).

We now possess the numerical algorithm for performing the bead–spring simulations, and the formula needed to calculate stress. It remains only to determine a reasonable value for the dimensionless spring constant K, a topic which is considered in the next section.

5. Estimating K

The above model of polymer structure is of course only a crude approximation to the true structure of a polymer. The model is for instance freely jointed whereas a true polymer has fixed bond angles, with (hindered) rotation about the bonds. The energies involved in distorting a polymer chain involve Coulomb interactions between large numbers of charged particles, much more complicated than the Fraenkel spring energies we have proposed. The hope is that for long polymer chains, these details will become of secondary importance by comparison to the sheer length of the chain, and the crude structure will then adequately describe the physics.

Given the crudeness of the model there do not exist tabulated values of the quantity K for various polymers, nor would such tables be particularly meaningful. Nonetheless appropriate order of magnitude estimates of K can be supplied, based on other polymer data. Useful data for this purpose consist of bond lengths, angles and energies, spectroscopic data and also solvent viscosities (Weast 1971–72; Kaye & Laby 1973; Herzberg 1945; Kirkwood & Slater 1931; Pitzer 1959; Abe *et al.* 1966; Flory 1969). Details of how these data can be used to estimate K are given in Grassia (1994).

The value of K one obtains depends to some extent on what physically constitutes the mathematical 'beads' and 'links' of the above model. If a link is supposed to consist of a single carbon–carbon bond then an appropriate value of K would be 2×10^3–10^4 (Grassia 1994). However it appears better to allow a link to consist of a group of several bonds (Abe *et al.* 1966; Flory 1969; Liu 1989). The spring energies in the model then arise from the van der Waals interactions of the various atoms comprising the link as they are rearranged into different geometries. The dimensionless spring constant K will be much smaller for a group of bonds than for a single bond, reflecting the small energy of van der Waals interactions compared with covalent carbon–carbon bonds. A typical value is $K \approx 34$ (Grassia 1994).

Regardless of whether we take beads and links to be composed of single bonds or groups of bonds it is clear that K is typically somewhat larger than 1. The random forcing leads to an 'equipartition of energy' (see Reif 1965; Grassia *et al.* 1995); for $K \gg 1$ the expected value of the spring energy in each link is $\frac{1}{2}$ in dimensionless units. The l_i will vary by a factor $\pm O(1/K^{1/2})$ about their natural value of unity. Since K is large, the available energy only extends or compresses the links by small amounts, or in other words the springs are quite stiff.

A related consequence is the fact that once the links are stretched or compressed, they will (in the absence of other forcing) return to their natural length in a short time $O(1/K)$. For stability in a numerical simulation it is necessary resolve this rapid relaxation process, requiring very small numerical time steps $\delta t < 1/K$. This rapid process however turns out to have no bearing on the evolution of parameters of rheological interest, e.g. the stress produced by the chain. Note that since $l_i - 1$ is $\pm O(1/K^{1/2})$, the tensions in the links $K(l_i - 1)$ are of magnitude $O(K^{1/2}) \gg 1$. However when we average the tensions over all link lengths l_i for a given configuration of link directions $\boldsymbol{d}_i$ we obtain a result independent of K. We are again faced with the difficulty of averaging many quantities of large magnitude, to determine an average of smaller magnitude.

Thus we wish to replace the bead–spring model by one in which the links are inextensible, i.e. rigid rods. The bead–rod model avoids the issue of link length relaxation, and permits us to choose time steps commensurate with the evolution of the stress relaxation phenomena we wish to observe. The only parameter remaining to govern the relaxation of the bead–rod model is the number of links n. Thus this model unambiguously addresses the question posed in §1 of how n affects the chain evolution.

6. Formulation of the bead–rod model

In this section we formulate the equations of the bead–rod model. As we shall see, it is necessary to introduce an additional force, which we call the pseudopotential force, to ensure that the bead–rod system mimics the statistics of the bead–spring system.

In the bead–rod model the link length $\hat{l}_i$ must be set to the natural length $\hat{l}$ or in dimensionless terms l_i must be set to unity. The tensions, rather than being given by the configuration, must be chosen to satisfy the constraint that the links are inextensible. If random forces $\boldsymbol{F}_i^{ra}$ act on the chain then the tensions will respond to these. Let us now denote the tensions by τ_i^{ra}, by contrast with the earlier bead–spring notation τ_i^{sp}. Then if the links are acted on by random forces $\boldsymbol{F}_i^{ra}$, the bead motion is

$$\dot{\boldsymbol{X}}_i = \boldsymbol{F}_i^{ra} + \tau_{i+1}^{ra}\boldsymbol{d}_{i+1} - \tau_i^{ra}\boldsymbol{d}_i,$$

so that $\dot{\boldsymbol{D}}_i \equiv \dot{\boldsymbol{X}}_i - \dot{\boldsymbol{X}}_{i-1}$ is

$$\dot{\boldsymbol{D}}_i = \boldsymbol{F}_i^{ra} - \boldsymbol{F}_{i-1}^{ra} + \tau_{i+1}^{ra}\boldsymbol{d}_{i+1} - 2\tau_i^{ra}\boldsymbol{d}_i + \tau_{i-1}^{ra}\boldsymbol{d}_{i-1}.$$

Inextensibility requires $\dot{\boldsymbol{D}}_i \cdot \boldsymbol{d}_i = 0$. Substituting for $\dot{\boldsymbol{D}}_i$ from the above we deduce

$$\boldsymbol{d}_i \cdot (-\tau_{i+1}^{ra}\boldsymbol{d}_{i+1} + 2\tau_i^{ra}\boldsymbol{d}_i - \tau_{i-1}^{ra}\boldsymbol{d}_{i-1}) = \boldsymbol{d}_i \cdot (\boldsymbol{F}_i^{ra} - \boldsymbol{F}_{i-1}^{ra}),$$

giving a tridiagonal system of equations to be solved for the tensions. Numerically this can be solved in $O(n)$ steps. Remember that $\boldsymbol{d}_i$ is a unit vector here, i.e. $\boldsymbol{d}_i \cdot \boldsymbol{d}_i \equiv 1$.

Thus we have

$$-\boldsymbol{d}_i \cdot \boldsymbol{d}_{i+1}\tau^{ra}_{i+1} + 2\tau^{ra}_i - \boldsymbol{d}_i \cdot \boldsymbol{d}_{i-1}\tau^{ra}_{i-1} = \boldsymbol{d}_i \cdot (\boldsymbol{F}^{ra}_i - \boldsymbol{F}^{ra}_{i-1}).$$

A suitable generalized coordinate set for describing the bead–rod chain configuration consists of the following two sets of variables: firstly the cosines of the angles between the links $-\boldsymbol{d}_i \cdot \boldsymbol{d}_{i\pm1}$, and secondly the azimuthal angle by which a link is rotated out of the plane spanned by the previous two links, the rotation being about the axis of the previous link. This angle is

$$\arccos\left((\boldsymbol{d}_{i+1} \cdot \boldsymbol{d}_{i-1} - \boldsymbol{d}_{i+1} \cdot \boldsymbol{d}_i \boldsymbol{d}_i \cdot \boldsymbol{d}_{i-1})/(1 - (\boldsymbol{d}_{i+1} \cdot \boldsymbol{d}_i)^2)^{1/2}(1 - (\boldsymbol{d}_{i-1} \cdot \boldsymbol{d}_i)^2)^{1/2}\right).$$

It is well documented in the literature (Kramers 1946; Kirkwood & Riseman 1956; Gottlieb & Bird 1976; Fixman 1978*a*; Rallison 1979; van Kampen 1981; Bird *et al.* 1987; Hinch 1994) that the equilibrium probability distribution of the bead–rod system written in terms of these variables is just the square root of the determinant of the tridiagonal matrix appearing in the equation to be solved for the tensions. For simplicity we shall denote this determinant by 'det'. For instance, in the much studied case of a trimer or trumbbell (3 beads, 2 links, $n = 2$) the determinant is $\det = 4 - (\boldsymbol{d}_1 \cdot \boldsymbol{d}_2)^2$, and the equilibrium distribution is $\sqrt{\det} = (4 - (\boldsymbol{d}_1 \cdot \boldsymbol{d}_2)^2)^{1/2}$. For longer bead–rod chains the equilibrium distribution $\sqrt{\det}$ is independent of the azimuthal angles. However there is a dependence on the cosines of the angles between the links. Bead–spring chains on the other hand are known to have a uniform distribution.

The reason for the difference in the probability distributions can be seen by first allowing non-zero bead masses and then taking a limit as bead mass vanishes. Writing the bead–rod system in terms of our generalized coordinates reveals that the generalized mass of the bead–rod system varies like det. The equilibrium probability distribution is $\sqrt{\det}$, favouring high-inertia configurations, since they explore more of momentum space for their allotted thermal energy. The actual value of the bead masses cancels in the normalization, so that the $\sqrt{\det}$ distribution continues to hold in the limit of vanishing bead mass.

Physically, the bead–rod system is not the $K \to \infty$ limit of a system with spring energy $\sum_{i=1}^{n} \frac{1}{2}K(l_i - 1)^2$, but rather the $K \to \infty$ limit of a system with an energy formula $\sum_{i=1}^{n} \frac{1}{2}K(l_i - 1)^2/\det^{1/n}$. For $l_i = 1$ both these formulae give zero energy. We believe that it is physically unrealistic to have a spring stiffness varying with the configuration of the link directors $\boldsymbol{d}_i$ like $\det^{1/n}$. This is because det depends on the totality of directors, even those for links located far away from a given spring. In short we believe that the bead–rod system is physically wrong.

In order make the bead–rod system behave like the physically correct bead–spring system, it is necessary to add additional forces, repelling the beads from those configurations where det is large (Fixman 1978*a*; Hinch 1994). The forces required, denoted $\boldsymbol{F}^{ps}_i$, can be derived from an additional potential energy $\log\sqrt{\det}$. We call this additional energy a pseudopotential, and we define pseudopotential forces as $\boldsymbol{F}^{ps}_i = -\nabla_i \log\sqrt{\det}$. Fortunately for a chain of n links these forces can be found in $O(n)$ operations. From a numerical point of view, this is an advantage, since calculating the $\boldsymbol{F}^{ps}_i$ does not lead to massive increases in the amount of computation for each time step. For details, see the Appendix.

We must also introduce pseudopotential tensions, τ^{ps}_i say. These satisfy

$$-\boldsymbol{d}_i \cdot \boldsymbol{d}_{i+1}\tau^{ps}_{i+1} + 2\tau^{ps}_i - \boldsymbol{d}_i \cdot \boldsymbol{d}_{i-1}\tau^{ps}_{i-1} = \boldsymbol{d}_i \cdot (\boldsymbol{F}^{ps}_i - \boldsymbol{F}^{ps}_{i-1}).$$

Tensions are linear in the forcing so the introduction of the $\boldsymbol{F}_i^{ps}$ does not affect the definition of τ_i^{ra} given earlier.

The equation of motion of the beads is now

$$\dot{\boldsymbol{X}}_i = \boldsymbol{F}_i^{ra} + \tau_{i+1}^{ra}\boldsymbol{d}_{i+1} - \tau_i^{ra}\boldsymbol{d}_i + \boldsymbol{F}_i^{ps} + \tau_{i+1}^{ps}\boldsymbol{d}_{i+1} - \tau_i^{ps}\boldsymbol{d}_i.$$

7. Bead–rod numerical algorithm

There are two remaining barriers to solving the above equation of motion numerically. Firstly a midpoint stepping scheme must be used (Fixman 1978*a*; Grassia *et al.* 1995). This is a consequence of the variation of the generalized friction and generalized diffusivity when the bead–rod system is written in generalized coordinates. A drift is produced in the Brownian motion, and the numerical scheme must obtain the same drift. The requirement of using a midpoint rule is well known in the stochastic calculus literature, where it is referred to as the Stratonovich formulation (Kloeden & Platen 1980; Øskendal 1985).

Secondly, since friction appears in the fluctuation-dissipation theorem, the variation of the bead–rod (generalized) friction, implies that it is no longer correct to choose random forces $(6/\delta t)^{1/2}\boldsymbol{n}_i$. It is necessary instead to choose random forces reflecting the link length constraints, and there are various ways to do this. Ermak & McCammon (1978) have suggested a procedure, which amounts to expressing the friction of all the beads in the form of a matrix and then carrying out a Choleski factorization. For numerical purposes a better scheme is that of Hinch (1994), since it involves fewer numerical operations. In this latter scheme, firstly unconstrained random forces $\boldsymbol{F}_i^{ra\ (uncon)}$ are taken to be $(6/\delta t)^{1/2}\boldsymbol{n}_i$. Then constraining tensions $\tau_i^{ra\ (con)}$ are calculated satisfying

$$-\boldsymbol{d}_i\cdot\boldsymbol{d}_{i+1}\tau_{i+1}^{ra\ (con)} + 2\tau_i^{ra\ (con)} - \boldsymbol{d}_i\cdot\boldsymbol{d}_{i-1}\tau_{i-1}^{ra\ (con)} = \boldsymbol{d}_i\cdot(\boldsymbol{F}_i^{ra\ (uncon)} - \boldsymbol{F}_{i-1}^{ra\ (uncon)}).$$

The random forces required are $\boldsymbol{F}_i^{ra} = \boldsymbol{F}_i^{ra\ (uncon)} + \tau_{i+1}^{ra\ (con)}\boldsymbol{d}_{i+1} - \tau_i^{ra\ (con)}\boldsymbol{d}_i$.

We can now explicitly give the numerical algorithm for performing a time step. We again employ the notation that $()_0$, $()_{1/2}$ and $()_1$ denote values at the beginning, midpoint and end of a time step. The random forces active during the step are $(\boldsymbol{F}_i^{ra})_0$. Note that the construction of $(\boldsymbol{F}_i^{ra})_0$ implies that $(\tau_i^{ra})_0$ vanish.

This fact has implications for the values of $(\tau_i^{ra})_{1/2}$ and $(\tau_i^{ra})_1$, which are the tensions produced by $(\boldsymbol{F}_i^{ra})_0$ at respectively the midpoint and end of the time step. These tensions are products of $O(1/(\delta t)^{1/2})$ forces with $O((\delta t)^{1/2})$ configuration changes during a time step, and thus are $O(1)$, not $O(1/(\delta t)^{1/2})$ quantities. The case of $(\tau_i^{ra})_1$ is particularly important since it will appear in the numerical implementation of the stress formula, to be considered in the next section. As in §4 it is vastly easier to determine an $O(1)$ average of $O(1)$ values, rather than an $O(1)$ average of $O(1/(\delta t)^{1/2})$ quantities.

The numerical scheme is

$$(\boldsymbol{X}_i)_{1/2} = (\boldsymbol{X}_i)_0 + \frac{\delta t}{2}\Big((\boldsymbol{F}_i^{ra})_0 + (\boldsymbol{F}_i^{ps})_0 + (\tau_{i+1}^{ps})_0(\boldsymbol{d}_{i+1})_0 - (\tau_i^{ps})_0(\boldsymbol{d}_i)_0\Big),$$

$$(\boldsymbol{X}_i)_1 = (\boldsymbol{X}_i)_0 + \delta t\Big((\boldsymbol{F}_i^{ra})_0 + (\tau_{i+1}^{ra})_{1/2}(\boldsymbol{d}_{i+1})_{1/2} - (\tau_i^{ra})_{1/2}(\boldsymbol{d}_i)_{1/2} + (\boldsymbol{F}_i^{ps})_{1/2} + (\tau_{i+1}^{ps})_{1/2}(\boldsymbol{d}_{i+1})_{1/2} - (\tau_i^{ps})_{1/2}(\boldsymbol{d}_i)_{1/2}\Big).$$

This numerical scheme possesses truncation error and therefore will not maintain

exact inextensibility of the links. However the link directors $\boldsymbol{d}_i$ are unit vectors by construction, and so can be used to reset the bead positions $\boldsymbol{X}_i$, restoring link lengths to unity. In our numerical scheme we carry out this procedure whenever the link lengths deviate from 1 by more than 0.5%. Liu (1989) has performed simulations with an alternative numerical scheme which always maintains link inextensibility within any desired tolerance, thereby avoiding the need to reset bead positions. The disadvantage of Liu's scheme is that a nonlinear equation for the tensions must be solved at each time step.

8. Bead–rod formula for stress

The numerical algorithm has been specified, and it remains to give a numerical implementation of the Kramers stress formula. Care must be exercised here owing to the discontinuity of the random forcing from time step to time step. Liu (1989) has considered stress formulae for a bead–rod chain in an applied flow field, but used simulations only to calculate the equilibrium stress. Thus he obtained a stress formula involving the flow field and the configuration of the beads, but not the random forcing. In the present paper however we wish to investigate the unsteady stress evolution of a chain, with no applied flow, and for this the random forcing needs to contribute to the stress formula.

Indeed the stress $\boldsymbol{\sigma}$ can be separated into a part depending on the random forcing and a part depending on the pseudopotential. We denote these $\boldsymbol{\sigma}_{ra}$ and $\boldsymbol{\sigma}_{ps}$ respectively. We have

$$\boldsymbol{\sigma}_{ra} = -\sum_{i=0}^{n} \tfrac{1}{2}\langle((\boldsymbol{X}_i)_1 - (\boldsymbol{X}_i)_0)(\boldsymbol{F}_i^{ra})_0\rangle + \sum_{i=1}^{n} \tfrac{1}{2}\langle(\tau_i^{ra})_1(l_i)_1(\boldsymbol{d}_i)_1(\boldsymbol{d}_i)_1\rangle.$$

The first term is identical to $\boldsymbol{\sigma}_{ra}$ in the bead–spring stress formula. The factor $\frac{1}{2}$ in the second term arises since at the end of the time step the tensions τ_i^{ra} change discontinuously from $(\tau_i^{ra})_1$ to 0. In future sections shall employ the symbol $(\tau_i^{ra\ (ave)})_1$ to represent the average of these two values, which is $\frac{1}{2}(\tau_i^{ra})_1$. The term $(l_i)_1$ in the stress formula is ideally unity, but may differ slightly from 1 owing to truncation errors. Resetting the link lengths back to unity will make negligible changes to the stress, in practice much less than statistical fluctuations.

The pseudopotential contribution to the stress $\boldsymbol{\sigma}_{ps}$ in the configuration $(\boldsymbol{X}_i)_1$ is given straightforwardly by

$$\boldsymbol{\sigma}_{ps} = -\sum_{i=0}^{n}\langle(\boldsymbol{X}_i)_1(\boldsymbol{F}_i^{ps})_1\rangle + \sum_{i=1}^{n}\langle(\tau_i^{ps})_1(l_i)_1(\boldsymbol{d}_i)_1(\boldsymbol{d}_i)_1\rangle.$$

This completes our description of the numerical method for bead–rod chains. In subsequent sections we shall employ this method to investigate a problem of rheological interest: the relaxation of stress in an initially straight polymer chain.

9. Stress in an exactly straight chain

We now possess the numerical formulae needed to investigate stress evolution in both bead–spring chains (§4) and bead–rod chains (§8). This is an appropriate point to describe briefly the structure of the remainder of the paper. Our ultimate aim is to study the stress evolution in a problem of rheological interest: the relaxation of stress in an initially straight polymer chain. In this section we shall describe the

stress evolution we expect, deriving a formula for the initial stress. The formula to be obtained has an important physical interpretation, which we shall discuss in the next section. Then we shall confirm for short chains that both the bead–spring and bead–rod models bear out the expected stress evolution. Having established this, there will be no further need to consider bead–spring chains, and thereafter we shall focus exclusively on the bead–rod model, treating considerably longer chains.

Let there be Cartesian coordinate vectors $\boldsymbol{e}_1$, $\boldsymbol{e}_2$ and $\boldsymbol{e}_3$. Imagine an initially exactly straight bead–rod chain stretched along the $\boldsymbol{e}_1$ direction,

$$(\boldsymbol{X}_i)_0 = \left(i - \frac{n}{2}\right)\boldsymbol{e}_1, \quad (\boldsymbol{D}_i)_0 = (\boldsymbol{d}_i)_0 = \boldsymbol{e}_1.$$

Physically this configuration corresponds to stretching the chain by a very strong flow, and then switching off the flow. We aim to calculate the stress at the instant the flow is switched off.

Following the formula given in the previous section, we must perform one numerical time step, and calculate the stress at the end of this time step.

The pseudopotential forces involve gradients of dot products of the unit link directors $\boldsymbol{d}_i$. Since the $\boldsymbol{d}_i$ are by construction unit vectors, they are normal to their gradients. However if all the $\boldsymbol{d}_i$ are in the same direction, then the gradient of any one of them is normal to every unit link director. Hence the $\boldsymbol{F}_i^{ps}$ all vanish in the exactly straight configuration. Moreover the drift terms (Hinch 1994), which ordinarily necessitate the use of a midpoint stepping scheme, can also be shown to vanish for the straight configuration. Hence for the present stress calculation we need only consider a simple forward time step ignoring pseudopotentials.

Given unconstrained random forcing on bead i, $\boldsymbol{F}_i^{ra\ (uncon)} = (6/\delta t)^{1/2}\boldsymbol{n}_i$, the (actual) random forces $\boldsymbol{F}_i^{ra}$ are simple to calculate for a straight chain. In directions normal to the $\boldsymbol{e}_1$ direction, the components of $\boldsymbol{F}_i^{ra}$ are precisely the same as those of $\boldsymbol{F}_i^{ra\ (uncon)}$. For bead i, we shall denote this sideways random force by $(6/\delta t)^{1/2}\boldsymbol{n}_i'$ where we have defined $\boldsymbol{n}'_i = (\boldsymbol{I} - \boldsymbol{e}_1\boldsymbol{e}_1)\cdot\boldsymbol{n}_i$. Along the $\boldsymbol{e}_1$ direction the component of $\boldsymbol{F}_i^{ra}$ is the same for each bead, and is $(6/\delta t)^{1/2}\sum_{j=0}^{n}\boldsymbol{n}_j\cdot\boldsymbol{e}_1\boldsymbol{e}_1/(n+1)$. Hence

$$(\boldsymbol{F}_i^{ra})_0 = \left(\frac{6}{\delta t}\right)^{1/2}\left(\boldsymbol{n}_i' + \frac{1}{n+1}\sum_{j=0}^{n}\boldsymbol{n}_j\cdot\boldsymbol{e}_1\boldsymbol{e}_1\right).$$

In the above we have put $()_0$ around $\boldsymbol{F}_i^{ra}$ to indicate that this is a force acting between times 0 and δt.

The simple forward time step gives

$$(\boldsymbol{X}_i)_1 = \left(i - \frac{n}{2}\right)\boldsymbol{e}_1 + (6\delta t)^{1/2}\left(\boldsymbol{n}_i' + \frac{1}{n+1}\sum_{j=0}^{n}\boldsymbol{n}_j\cdot\boldsymbol{e}_1\boldsymbol{e}_1\right).$$

$$(\boldsymbol{D}_i)_1 = \boldsymbol{e}_1 + (6\delta t)^{1/2}(\boldsymbol{n}_i' - \boldsymbol{n}_{i-1}').$$

The link director $(\boldsymbol{d}_i)_1$ is $(\boldsymbol{D}_i)_1/[1 + 6\delta t\,(\boldsymbol{n}_i' - \boldsymbol{n}_{i-1}')\cdot(\boldsymbol{n}_i' - \boldsymbol{n}_{i-1}')]^{1/2}$.

The tensions $(\tau_i^{ra})_1$ are obtained by solving the tridiagonal tension equation given in §6. At leading order in the time step δt we may replace the right-hand side of the tension equation $(\boldsymbol{d}_i)_1\cdot((\boldsymbol{F}_i^{ra})_0 - (\boldsymbol{F}_{i-1}^{ra})_0)$ by $6(\boldsymbol{n}_i' - \boldsymbol{n}_{i-1}')\cdot(\boldsymbol{n}_i' - \boldsymbol{n}_{i-1}')$, and also replace $(\boldsymbol{d}_i)_1\cdot(\boldsymbol{d}_{i\pm1})_1$ on the left-hand side by 1. We take expectations to obtain

$$-\langle(\tau_{i+1}^{ra})_1\rangle + 2\langle(\tau_i^{ra})_1\rangle - \langle(\tau_{i-1}^{ra})_1\rangle = 6\langle(\boldsymbol{n}_i' - \boldsymbol{n}_{i-1}')\cdot(\boldsymbol{n}_i' - \boldsymbol{n}_{i-1}')\rangle.$$

On the left-hand side of the above equation we have a tridiagonal matrix with 2's

down the diagonal and -1's above and below. In the literature this is called the Rouse matrix. We shall let its inverse, which is known as the Kramers matrix, be denoted Λ_{ij}. It is well known (see e.g. Rallison 1979) that

$$\Lambda_{ij} = \begin{cases} (n+1-i)j/(n+1), & i \geqslant j, \\ (n+1-j)i/(n+1), & i \leqslant j, \end{cases}$$

and hence

$$\langle (\tau_i^{ra})_1 \rangle = 6\Lambda_{ij} \langle (\boldsymbol{n}_j' - \boldsymbol{n}_{j-1}') \cdot (\boldsymbol{n}_j' - \boldsymbol{n}_{j-1}') \rangle,$$

with summation over j on the right-hand side. Now using the facts that $\langle \boldsymbol{n}_i' \boldsymbol{n}_i' \rangle = (\boldsymbol{I} - \boldsymbol{e}_1\boldsymbol{e}_1)/3$, that $\langle \boldsymbol{n}_i \boldsymbol{n}_j \rangle$ vanishes when $i \neq j$ and that $\sum_j \Lambda_{ij} = \frac{1}{2}(n+1-i)i$, we deduce $\langle (\tau_i^{ra})_1 \rangle = 4(n+1-i)i$. Recalling the definition of $(\tau_i^{ra\ (ave)})_1$ in the previous section, we note for future reference that

$$\langle (\tau_i^{ra\ (ave)})_1 \rangle \equiv \tfrac{1}{2} \langle (\tau_i^{ra})_1 \rangle = 2(n+1-i)i.$$

Thus the average tension in link i of a straight chain is $2(n+1-i)i$.

The stress contribution arising from the $(\tau_i^{ra})_1$ terms is

$$\sum_{i=1}^{n} \tfrac{1}{2} \langle (\tau_i^{ra})_1 (l_i)_1 (\boldsymbol{d}_i)_1 (\boldsymbol{d}_i)_1 \rangle,$$

which to leading order is

$$\sum_{i=1}^{n} \tfrac{1}{2} \langle (\tau_i^{ra})_1 \rangle \boldsymbol{e}_1\boldsymbol{e}_1 = \sum_{i=1}^{n} 2(n+1-i)i\, \boldsymbol{e}_1\boldsymbol{e}_1.$$

This equals $n(\frac{1}{3}n^2 + n + \frac{2}{3})\boldsymbol{e}_1\boldsymbol{e}_1$.

The stress $\boldsymbol{\sigma}_{ra}$ has an additional contribution

$$-\sum_{i=0}^{n} \tfrac{1}{2} \langle ((\boldsymbol{X}_i)_1 - (\boldsymbol{X}_i)_0)(\boldsymbol{F}_i^{ra})_0 \rangle = -\sum_{i=0}^{n} \langle (\boldsymbol{F}_i^{ra})_0 (\boldsymbol{F}_i^{ra})_0 \rangle \frac{\delta t}{2}.$$

In the $\boldsymbol{e}_1\boldsymbol{e}_1$ direction this gives

$$\sum_{i=0}^{n} \left\langle \left(\frac{1}{n+1} \left(\frac{6}{\delta t} \right)^{1/2} \sum_{j=0}^{n} \boldsymbol{n}_j \cdot \boldsymbol{e}_1 \boldsymbol{e}_1 \right) \left(\frac{1}{n+1} \left(\frac{6}{\delta t} \right)^{1/2} \sum_{k=0}^{n} \boldsymbol{n}_k \cdot \boldsymbol{e}_1 \boldsymbol{e}_1 \right) \right\rangle \frac{\delta t}{2} = -\boldsymbol{e}_1\boldsymbol{e}_1,$$

whilst in the $\boldsymbol{I} - \boldsymbol{e}_1\boldsymbol{e}_1$ direction it yields

$$-\sum_{i=0}^{n} \left\langle \left(\frac{6}{\delta t} \right)^{1/2} \boldsymbol{n}_i' \left(\frac{6}{\delta t} \right)^{1/2} \boldsymbol{n}_i' \right\rangle \frac{\delta t}{2} = -(n+1)(\boldsymbol{I} - \boldsymbol{e}_1\boldsymbol{e}_1).$$

We conclude for an exactly straight chain that

$$\begin{aligned} \boldsymbol{\sigma} = \boldsymbol{\sigma}_{ra} &= n\left(\tfrac{1}{3}n^2 + n + \tfrac{2}{3}\right)\boldsymbol{e}_1\boldsymbol{e}_1 - \boldsymbol{e}_1\boldsymbol{e}_1 - (n+1)(\boldsymbol{I} - \boldsymbol{e}_1\boldsymbol{e}_1) \\ &= n\left(\tfrac{1}{3}n^2 + n + \tfrac{5}{3}\right)\boldsymbol{e}_1\boldsymbol{e}_1 - (n+1)\boldsymbol{I}. \end{aligned}$$

This result is in dimensionless units. In dimensional units the bulk stress contribution of (exactly straight) chains would be $k\hat{T} \times \left(n\left(\frac{1}{3}n^2 + n + \frac{5}{3}\right)\boldsymbol{e}_1\boldsymbol{e}_1 - (n+1)\boldsymbol{I} \right)$. The calculation indicates that the stress in the exactly straight bead–rod chain is finite, unlike in some other polymer models, such as the entropic spring model (to be reviewed in §13), which give infinite stresses in exactly aligned chains. The finiteness

of the stress should be borne in mind when developing constitutive equations for polymeric solutions.

The above initial stress formula was based on calculating by hand the expectation value of the numerical formula given in §8. It is unnecessary to use the numerical formula of §8 as a starting point, and indeed there are a number of theoretical approaches which give the same end result. One approach is to consider a free sideways diffusion of the beads at early times, and deduce from this the rate at which the $\boldsymbol{e}_1$ component of the link directors decreases. This information can then be substituted into an alternative stress formula, the Gisekus formula (Bird *et al.* 1987) to give the above result. Another alternative (Grassia 1994) is to give the random forces in terms of the gradient of a logarithm of the probability distribution. Taking expectation values and integrating by parts, gives the desired stress formula. The various approaches do not necessarily agree with respect to the proportion of stress assigned separately to bead random forcing and to rod tensions, but the overall stress is always the same. In the next section we shall recalculate the link tensions using a specific theoretical approach, which clearly indicates the physical origin of the initial stress.

For exactly straight bead–spring chains, we cannot repeat the stress calculation culminating in the formula $\boldsymbol{\sigma} = n(\frac{1}{3}n^2 + n + \frac{5}{3})\boldsymbol{e}_1\boldsymbol{e}_1 - (n+1)\boldsymbol{I}$. This is because the correct initial stress for the bead–spring chain is only established on times longer than $O(1/K)$, the link length relaxation time. On the other hand numerical stability demands $\delta t < 1/K$, so the correct stress is only established after several time steps.

Thus far we have calculated the stress for (bead–rod) chains in the exactly straight configuration. We also wish to determine the stress for a randomly coiled chain, which will represent the end-point of the stress evolution. This calculation is trivial if we replace the Kramers stress formula by the equivalent alternative formula of Gisekus (Bird *et al.* 1987). The stress is found to be $-\boldsymbol{I}$ in dimensionless units, and corresponds to the chain supplying a pressure equivalent to that of a molecule in an ideal gas. The stress in a randomly coiled bead–spring chain is also $-\boldsymbol{I}$. Moreover the distribution of spring link lengths in such a chain will be governed by a Boltzmann factor involving the energy of the springs.

Summarizing then, we hope in our simulations to see an evolution of stress starting from $\boldsymbol{\sigma} = n(\frac{1}{3}n^2 + n + \frac{5}{3})\boldsymbol{e}_1\boldsymbol{e}_1 - (n+1)\boldsymbol{I}$ and finishing with $\boldsymbol{\sigma} = -\boldsymbol{I}$. Moreover we hope to find agreement between the stress in the bead–rod and bead–spring chains. The results from the simulations will be considered shortly; however before turning to these, it is helpful to describe the physical significance of the stress in the straight chain.

10. Physical interpretation of stress

The bead–rod tensions have a simple physical purpose which was discussed at the beginning of §6: namely that they are of exactly the correct magnitude to maintain link inextensibility. In a straight chain it is particularly clear how the average link tensions calculated in the previous section $\langle(\tau_i^{ra\ (ave)})_1\rangle = 2(n+1-i)i$ achieve this inextensibility requirement, as we now explain. The issues we describe in this section will not only be useful for interpreting the initial value of the stress, but in future sections will help us to understand the early and intermediate time stress relaxation.

The chain is initially stretched along the $\boldsymbol{e}_1$ direction. For small values of t, the bead motion is predominately sideways in the $\boldsymbol{e}_2$ and $\boldsymbol{e}_3$ directions. We shall let $\boldsymbol{z}_i$ denote

the sideways position of bead i, and this is a random function of time t. Provided the magnitude of z_i is small compared with 1, then $\boldsymbol{d}_i \approx \boldsymbol{e}_1 + (z_i - z_{i-1})$.

As well as bead positions, we are also concerned with bead velocities. The sideways velocity of bead i is just $\dot{z}_i$. There is also a longitudinal velocity component to be considered. This arises from the tensions in the adjacent links, plus a longitudinal diffusion of chain centre of mass superposed. The links are assumed to lie almost exactly along the $\boldsymbol{e}_1$ direction, so that the longitudinal velocity of bead i is $(\tau^{ra}_{i+1} - \tau^{ra}_i)\,\boldsymbol{e}_1$ with respect to the centre of mass. Hence

$$\dot{\boldsymbol{D}}_i = (\tau^{ra}_{i+1} - 2\tau^{ra}_i + \tau^{ra}_{i-1})\,\boldsymbol{e}_1 + \dot{z}_i - \dot{z}_{i-1}.$$

The inextensibility requirement from §6 is $\dot{\boldsymbol{D}}_i \cdot \boldsymbol{d}_i = 0$, which gives

$$\tau^{ra}_{i+1} - 2\tau^{ra}_i + \tau^{ra}_{i-1} + \tfrac{1}{2}\frac{\mathrm{d}}{\mathrm{d}t}(z_i - z_{i-1}) \cdot (z_i - z_{i-1}) = 0.$$

The last term on the left-hand side represents the average rate at which the links would lengthen due to the sideways motion if there were no tensions. The first three terms represent the shortening of the links due to the tensions in the absence of sideways motion. The equation implies that the role of the tensions is to offset the tendency of the sideways motion to increase link lengths. Recalling the definition of the Kramers matrix A_{ij} in the previous section we have

$$\tau^{ra}_i = \tfrac{1}{2} A_{ij} \frac{\mathrm{d}}{\mathrm{d}t}(z_j - z_{j-1}) \cdot (z_j - z_{j-1}),$$

with summation over j. Taking expectation values yields

$$\langle \tau^{ra}_i \rangle = \tfrac{1}{2} A_{ij} \frac{\mathrm{d}}{\mathrm{d}t} \langle (z_j - z_{j-1}) \cdot (z_j - z_{j-1}) \rangle.$$

Now for very early times, the beads diffuse freely in the $\boldsymbol{e}_2$ and $\boldsymbol{e}_3$ directions, with unit diffusivity. We shall adopt a notation which looks very similar to that of the previous section. At time $t \ll 1$ the sideways position of bead i will be written $(6t)^{1/2} \boldsymbol{N}'_i$ where $\boldsymbol{N}'_i$ is a random sideways vector of vanishing mean and with variance $\langle \boldsymbol{N}'_i \boldsymbol{N}'_i \rangle = (\boldsymbol{I} - \boldsymbol{e}_1 \boldsymbol{e}_1)/3$. Moreover the beads move sideways independently so that $\langle \boldsymbol{N}'_i \cdot \boldsymbol{N}'_j \rangle$ vanishes if $i \neq j$. These facts all follow from the free diffusion, and also from adding together a total of $t/\delta t$ numerical time steps. We have therefore

$$\langle \tau^{ra}_i \rangle = 3 A_{ij} \langle (\boldsymbol{N}'_j - \boldsymbol{N}'_{j-1}) \cdot (\boldsymbol{N}'_j - \boldsymbol{N}'_{j-1}) \rangle.$$

Apart from a factor of $\frac{1}{2}$, and the notational change of $\boldsymbol{N}'_i$ replacing $\boldsymbol{n}'_i$, this is identical to the equation for $\langle (\tau^{ra}_i)_1 \rangle$ appearing in the previous section. The factor of $\frac{1}{2}$ can be absorbed by recalling that $\langle (\tau^{ra\ (ave)}_i)_1 \rangle$ is $\frac{1}{2} \langle (\tau^{ra}_i)_1 \rangle$.

Hence $\langle \tau^{ra}_i \rangle = \langle (\tau^{ra\ (ave)}_i)_1 \rangle = 2(n+1-i)i$. We have shown explicitly that the tensions in the straight chain $\langle (\tau^{ra\ (ave)}_i)_1 \rangle$ as calculated in §9 are of precisely the correct magnitude to maintain link inextensibility.

11. Comparing bead–rod and bead–spring chains

We start with some results for the trumbbell or trimer molecule. We considered both a bead–rod and bead–spring trumbbell, initially stretched straight along the $\boldsymbol{e}_1$ direction. In the bead–spring simulations, we considered two different values of the dimensionless spring constant, $K = 100$ and $K = 400$. Here we took initial values for

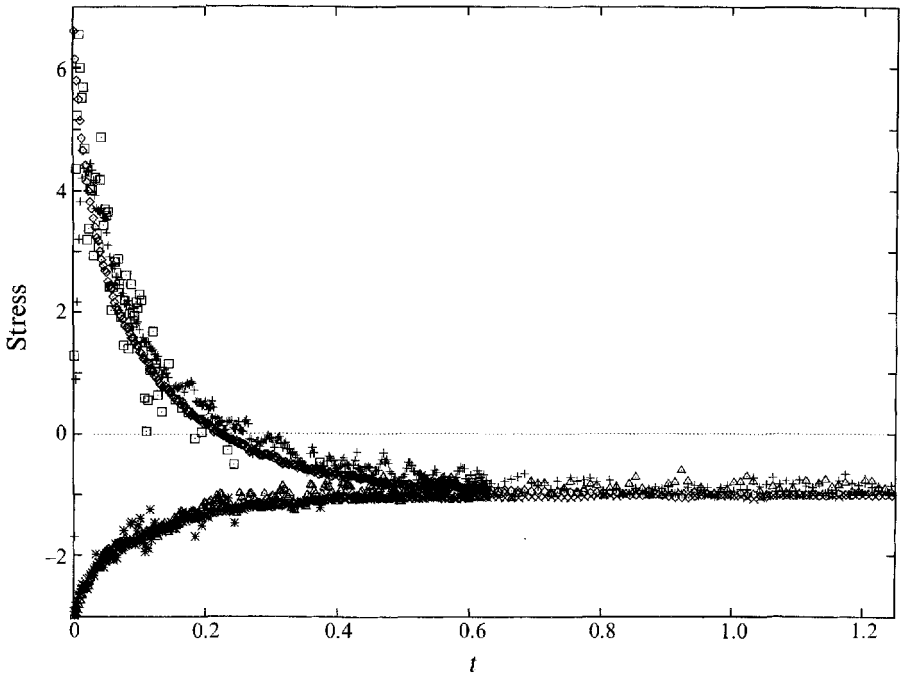

FIGURE 1. Trumbbell stress relaxation for stress components σ_{11} and σ_{22}. In the upper part of the graph we find σ_{11} data for a bead–rod trumbbell ◇ and for bead–spring trumbbells with $K = 100$ + and $K = 400$ □. In the lower part of the graph we find σ_{22} data for a bead–rod trumbbell ×, and for bead–spring trumbbells with $K = 100$ △ and $K = 400$ ✳. There were 4000 realizations in each case. The initial σ_{11} is 7, whilst the initial σ_{22} is -3. After time roughly $t = 0.5$ an isotropic equilibrium stress is attained with $\sigma_{11} = \sigma_{22} = -1$.

the lengths of the stiff spring links $l_1 = l_2 = 1$, so that the link tensions τ_1^{sp} and τ_2^{sp} both vanished at the initial instant.

The time step was $\delta t = 0.001$ for the bead–rod problem and also for the bead–spring problem with $K = 100$, but was $\delta t = 0.00025$ for the bead–spring problem with $K = 400$. Recall that the need for a small time step at large K was the very reason we developed the bead–rod model in §6.

The stress was calculated for each time step, but to reduce statistical fluctuations it was then averaged over several nearby time steps. The data were given as average stress over each group of several time steps *vs.* the mean time within the group. Finally an average was taken over 4000 realizations.

The results for the stress relaxation of the trumbbell are shown in figures 1 and 2. We plot the diagonal elements of stress, both in the $\boldsymbol{e}_1$ direction, along which the chain is initially aligned, and the $\boldsymbol{e}_2$ direction, which is one of the two directions normal to $\boldsymbol{e}_1$. We shall refer to these '11' and '22' stress components as σ_{11} and σ_{22} respectively.

Figure 1 shows the time evolution of σ_{11} and σ_{22} for a trumbbell starting from the initially straight chain configuration at $t = 0$, up to a time $t = 1.25$. Broadly there is agreement between the stress calculated by the bead–rod and bead–spring systems. Moreover the initial stress for the bead–rod trumbbell in the figure agrees with the predicted value from the previous section (with $n = 2$)

$$\boldsymbol{\sigma} = 10\boldsymbol{e}_1\boldsymbol{e}_1 - 3\boldsymbol{I} = 7\boldsymbol{e}_1\boldsymbol{e}_1 - 3(\boldsymbol{I} - \boldsymbol{e}_1\boldsymbol{e}_1).$$

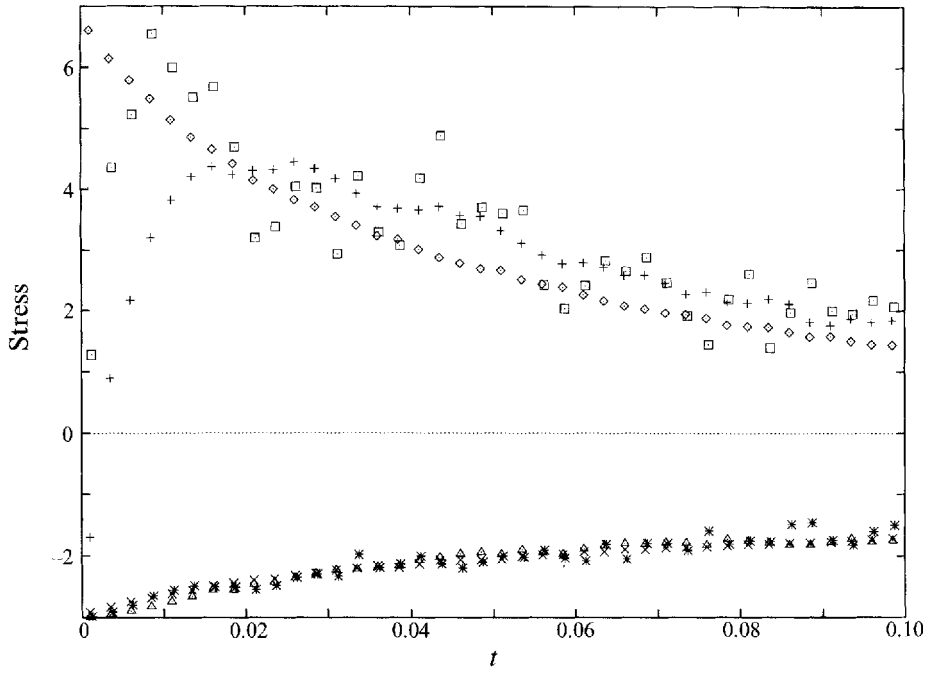

FIGURE 2. An expanded view of the initial part of figure 1. The stress σ_{11} in bead–spring models disagrees with that in bead–rod models for very early times. This arises from the artificial bead–spring initial condition $l_1 = l_2 = 1$ giving vanishing tension in the springy links. For times larger than $O(1/K)$ bead–spring and bead–rod models agree, the agreement being achieved somewhat sooner for spring constant $K = 400$ than for $K = 100$.

On figure 1 at time roughly $t = 0.5$, σ_{11} and σ_{22} both attain the equilibrium value -1.

Figure 2 shows an expanded view of the initial part of figure 1 on a finer scale. The most important point to note here is the failure of σ_{11} to agree in the bead–rod and bead–spring models at early times. This arises wholly from our artificial choice of $l_1 = l_2 = 1$ as the initial spring lengths, meaning τ_i^{sp} and σ_{sp} vanish initially. Having the wrong initial σ_{sp} does not influence σ_{22} since the springs do not initially lie along the '2' direction. Only σ_{11} is affected.

During a time $O(1/K)$, with $K \gg 1$, the unit link directors $\boldsymbol{d}_1$ and $\boldsymbol{d}_2$ are virtually unchanged from their initial values, but the artificial initial values of l_1 and l_2 are forgotten. After this period there ceases to be a discrepancy between the bead–rod and bead–spring stress relaxation. Note that the $K = 400$ bead–spring graph joins the bead–rod curve somewhat earlier than the $K = 100$ graph does, so our $O(1/K)$ estimate is indeed plausible.

We have investigated the energy stored in the stiff spring links. This is initially zero owing to our artificial initial conditions, but in time $O(1/K)$ it reaches the equilibrium value of $\frac{1}{2}$ per link. This value is demanded by equipartition of energy, and can be obtained via a Boltzmann distribution of link lengths. Hence we have discovered an important property of the bead–spring trumbbell: the link lengths and directions equilibrate essentially independently, the former on time scales $O(1/K)$ and the latter on $O(1)$ scales. The link lengths equilibrate to the Boltzmann distribution, whilst the relaxation of the link directions follows that of the bead–rod trumbbell. We emphasize that the dimensionless spring constant K is only defined for springs of non-zero natural length, since it compares the thermal energy with the energy

required to deform the springs by amounts comparable to their natural length. As we noted in §2, there is a diffusion time scale for link direction, defined in terms of the bead diffusivity and the natural link length, and this is independent of spring stiffness.

There is one minor modification to the picture of separate link length and link direction relaxation for our bead–spring models. During the bead–rod relaxation, the difference between the actual bead–rod stress in the '11' direction and the equilibrium value is positive. Thus the actual tensions in the rods must be on average positive and greater than the equilibrium values. In order for the bead–rod and bead–spring stress to agree, it is necessary for the springs to be on average slightly stretched with respect to a Boltzmann distribution. In other words the distribution of link lengths cannot be a perfect Boltzmann distribution, until the link directions have fully relaxed. However the departure from the Boltzmann distribution is small. An $O(1)$ stress in the links can be produced with $l_i - 1 = O(1/K)$, whilst under the Boltzmann distribution $l_i - 1$ fluctuates by larger $\pm O(1/K^{1/2})$ amounts. The energy involved in giving an extra $O(1/K)$ stretch to the springs is negligible compared with the equipartition energy.

Another point which is clear from figure 2 is that there is rather more scatter in the $\boldsymbol{\sigma}_{11}$ data for the bead–spring models, than for the bead–rod models. This arises from the $\boldsymbol{\sigma}_{sp}$ part of the stress formula (we consider times larger than $O(1/K)$). The tensions in the links will be $\pm O(K^{1/2})$, and we are faced with the statistical difficulty of averaging quantities of large magnitude to extract a smaller magnitude average. We anticipated this effect in §5. There is no large scatter in the bead–spring $\boldsymbol{\sigma}_{22}$ data at early times, since the links are aligned so that $\boldsymbol{\sigma}_{sp}$ has only a small '22' component.

The results we have described here are for the trumbbell. We have performed analogous simulations for bead–rod and bead–spring chains with $n = 4$. The same features occur, namely the stresses in the bead–spring and bead–rod chains agree, except for an initial $O(1/K)$ period, during which bead–spring link lengths equilibrate in energy. We anticipate that these features will be reproduced for a chain of any length provided the time scales for changes in the spring lengths remain short compared to the scales for evolution of link direction. We can therefore confidently discard the bead–spring model, and focus henceforth on bead–rod chains.

12. Relaxation of polymer chains: short time scales

We are now ready to investigate the primary question posed in this paper: How does the presence of a (typically large) number of links affect the process of chain relaxation? We shall consider the behaviour of the chain first at short time scales, then at long time scales, and finally will try to find a matching between the two. We are interested in the evolution of stress and we focus on the $\boldsymbol{\sigma}_{11}$ stress component (rather than say the $\boldsymbol{\sigma}_{22}$ component) since $\boldsymbol{\sigma}_{11}$ is known to fall from an $O(n^3)$ initial value, whereas $|\boldsymbol{\sigma}_{22}|$ decays only from an initial value $n+1$. Thus the $\boldsymbol{\sigma}_{11}$ decay is far more dramatic.

For a chain of length n we already know that there are initially $O(n^2)$ link tensions associated with the initial $O(n^3)$ stress. We estimate the time scale on which the stress will start to relax as follows.

As in §10 we denote the sideways position of bead i by z_i. We suppose that stress relaxes significantly whilst the links are still directed primarily along the $\boldsymbol{e}_1$ direction, i.e. while the magnitude of $z_i - z_{i\pm1}$ remains small. This permits us to use the tension formula (§10)

$$\langle \tau_i^{ra} \rangle = \tfrac{1}{2} A_{ij} \frac{\mathrm{d}}{\mathrm{d}t} \langle (z_j - z_{j-1}) \cdot (z_j - z_{j-1}) \rangle,$$

and the stress is essentially obtained by summing over these tensions. The right-hand side of this equation is a weighted sum of the difference in the rates of sideways motion for adjacent beads. For very early times the beads in the chain diffuse sideways independently so that the right-hand side is roughly $\frac{1}{2}A_{ij}(\mathrm{d}\langle z_j \cdot z_j\rangle/\mathrm{d}t + \mathrm{d}\langle z_{j-1} \cdot z_{j-1}\rangle/\mathrm{d}t)$. Clearly if we can reduce $\mathrm{d}\langle z_i \cdot z_i\rangle/\mathrm{d}t = 2\langle \dot{z}_i \cdot z_i\rangle$, we can reduce the tension and hence the stress.

Now $\dot{z}_i$ consists of one part due to the sideways diffusive force, plus another part from the tensions. We consider them in turn. In the absence of tensions, the sideways diffusive force would lead to $\mathrm{d}\langle z_i \cdot z_i\rangle/\mathrm{d}t = 4$ and hence $\langle \dot{z}_i z_i\rangle = 2$. The diffusive force can thus be estimated as $2z_i/(z_i \cdot z_i)$. The tension forces primarily act longitudinally, but they have a smaller sideways component arising from transverse projections of the link directions. The sideways tension force on bead i is $\tau^{ra}_{i+1}(z_{i+1} - z_i) - \tau^{ra}_i(z_i - z_{i-1})$. The beads diffuse independently early on, and so averaging this expression for force on bead i over the positions of beads $i \pm 1$ gives $-(\tau^{ra}_{i+1} + \tau^{ra}_i)z_i$.

The diffusive force acts to increase the magnitude of z_i, whilst the tension force acts to reduce it. Initially the diffusive force is much larger than the sideways tension force, however the former decreases and the latter increases as $\mathbf{z}_i$ grows. When these forces balance, the free sideways diffusion is arrested, the growth rate of z_i decreases, and hence so do the tension and stress. Balance occurs when $z_i \cdot z_i = 2/(\tau^{ra}_i + \tau^{ra}_{i-1})$. Using the relation from free diffusion $\langle z_i \cdot z_i\rangle = 4t$, and the fact that the expectation values of the τ^{ra}_i's are $O(n^2)$, we predict that the stress will start to relax on $O(1/n^2)$ time scales. In dimensional units, the relevant time scale is $O(\hat{\zeta}\hat{l}^2/k\hat{T} \times 1/n^2)$. The idea that tensions limit the sideways bead diffusion will be developed further in a later section.

In the first set of simulations, we have considered the stress relaxation on short time scales, looking only at the first decade of the stress decay. Thus in general we halted the simulations well before equilibrium is attained. We took values $n = 100$, $n = 50$, $n = 40$, $n = 20$ and $n = 16$. The time step was $0.004/n^2$. For the first 20 time steps we plotted the stress on every 4th step and thereafter we plotted on every 50th time step. This procedure was designed to ensure that when we plotted the stress evolution the graphs did not look too crowded. Of course a great deal of data available for the plot were discarded by not using stress data from every time step. Nonetheless, given that the stress evolves quite rapidly at these early times, discarding data was considered to be preferable to averaging stress over groups of time steps. A total of 1000 realizations was performed.

For each time at which the stress $\boldsymbol{\sigma}_{11}$ was sampled, we subtracted from $\boldsymbol{\sigma}_{11}$ the value -1, i.e. we subtracted the '11' component of the final equilibrium stress. Then we divided by $n\left(\frac{1}{3}n^2 + n + \frac{2}{3}\right)$ which is the difference between the '11' components of the initial and final stress.

In figure 3 we plot this 'fractional stress' $(\boldsymbol{\sigma}_{11} + 1)/\left(n\left(\frac{1}{3}n^2 + n + \frac{2}{3}\right)\right)$ against n^2t for various n in a log-linear plot. Notice that for $t \to 0$ in the graph the fractional stress has the value 1, implying that the initial stress formula derived in §9 is indeed valid. Also the curves for different n collapse almost onto a single curve, meaning our anticipated $O(1/n^2)$ time scale for relaxation is borne out. The fact that the curves with lower n lie slightly beneath those for higher n can be attributed to the finiteness of n. Indeed we could have taken just the leading-order approximation to $\boldsymbol{\sigma}_{11}$, namely $\frac{1}{3}n^3$, and plotted simply $(\boldsymbol{\sigma}_{11} + 1)/\left(\frac{1}{3}n^3\right)$. Then the situation would be reversed, with the curves for high n slightly beneath those for lower n.

The curve onto which the data collapse in figure 3 is certainly not a straight line, meaning that there is no single exponential for the short time decay. Instead there

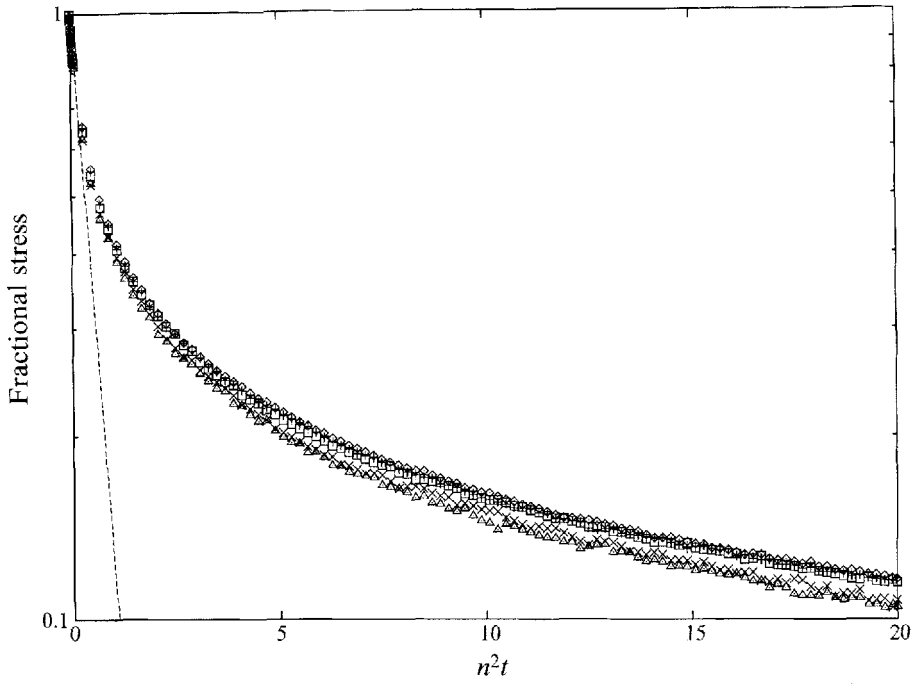

FIGURE 3. Relaxation of the fractional stress component $(\sigma_{11}+1)/\left(n\left(\frac{1}{3}n^2+n+\frac{2}{3}\right)\right)$ on short time scales. We have used values $n = 100$ ◇, $n = 50$ +, $n = 40$ □, $n = 20$ × and $n = 16$ △, with 1000 realizations in each case. Plotting against n^2t instead of t collapses the data onto a single curve, and indicates that relaxation rates scale like n^2. The fastest relaxation rate is $2.1\,n^2$, so that at very early times, the data are tangent to the line $\exp(-2.1\,n^2t)$ (dashed).

must be a spectrum of decay rates and those that govern the first decade of the stress decay must all have rate constants $O(n^2)$. The most rapid decay rate can be obtained from the slope of the graph as $t \to 0$. The best fit slope for $0 \leqslant n^2t \leqslant 0.1$ (where we have 25 data points) with $n = 100$ gives the highest rate constant as $2.1\,n^2$.

13. Entropic spring model

Now we turn to the stress relaxation on long time scales. In this section we shall review a crude model for the stress in the polymer chain. In the next section we shall review a more sophisticated model which yields quantitative predictions for the stress. After that we shall compare the numerical data for the bead–rod chain with the quantitative predictions of the model. As before we focus on the stress component σ_{11}. It is noteworthy that the models for stress relaxation on long time scales involve the decay of the longitudinal extension of the chain, with associated longitudinal bead motion. By contrast those for short time scale relaxation, such as that considered in the previous section, involve mainly sideways bead motion. On short time scales longitudinal motion does occur, but it only serves to maintain link inextensibility whenever adjacent beads move sideways at different rates. At some intermediate time, the chain must depart from straightness sufficiently to allow a change from predominately sideways bead motion to predominately longitudinal motion.

The model we consider first is called the 'entropic spring' model (Flory 1969). It

expresses the fact that aligning the links of a bead–rod chain has an entropy cost or equivalently a free energy cost. Let us denote the end-to-end vector of a chain by $\boldsymbol{R}$ (measured in units of a link length), and its expectation value by $\langle \boldsymbol{R} \rangle$. Clearly $\langle \boldsymbol{R} \rangle$ will vanish for a chain in equilibrium with no forces applied. Applying a force, $\boldsymbol{F}_{app}$ say, across the chain will give a non-vanishing $\langle \boldsymbol{R} \rangle$ at equilibrium. We suppose that $\boldsymbol{F}_{app}$ is measured in units of $k\hat{T}/\hat{l}$. Flory (1969) shows that $\langle \boldsymbol{R} \rangle$ is in the same direction as $\boldsymbol{F}_{app}$, and its magnitude (in dimensionless units) satisfies $|\langle \boldsymbol{R} \rangle|/n = \coth |\boldsymbol{F}_{app}| - 1/|\boldsymbol{F}_{app}|$. The right-hand side of this equation is a Langevin function in $|\boldsymbol{F}_{app}|$, so that applied force is an inverse Langevin function of expected chain length expressed as a fraction of the fully stretched length.

Flory (1969) surmises that a restoring force (denoted $\boldsymbol{F}$ say) inherent in the bead–rod chain must balance the applied force $\boldsymbol{F} = -\boldsymbol{F}_{app}$. Approximately then a chain with a non-zero $\boldsymbol{R}$ must have a restoring force given by the inverse Langevin force. This force arises from the increase in entropy as $|\boldsymbol{R}|$ decreases, and so is called an 'entropic force', whilst the bead–rod chain is said to behave like an 'entropic spring'. The stress of the entropic spring is $-\boldsymbol{RF} - 2\boldsymbol{I}$, the $-2\boldsymbol{I}$ term accounting for random forcing at each end of the spring unrelated to the entropic restoring force.

It is worth describing some of the deficiencies of this model and how they arise. For a chain with a given configuration of the link directors, it is (in principle) possible to average over all random forces and deduce the stress as a function of the link directors. Knowledge of the end-to-end vector alone is insufficient to determine the stress; the totality of link directors must be known. Averaging the stress over all configurations of link directors subject to a given end-to-end vector will not in general agree with the stress of the entropic spring.

One situation where the entropic spring model is clearly wrong is for an exactly straight chain. Here the inverse Langevin force is infinite. This is clear, since if the force applied across the chain were finite, there would always be small sideways deviation of the beads, and $|\langle \boldsymbol{R} \rangle|/n$ would be less than unity. However the stress for an exactly straight chain is known to be finite (deduced in §9 and verified in §12). Loosely speaking the error in the entropic spring model arises because the expected stress given a configuration is not the same thing as the stress (strictly the force) required to maintain a given expected configuration.

If $|\boldsymbol{R}|/n$ is not too close to unity, i.e. if the chain is not too close to being fully stretched, the inverse Langevin force can be linearized and the entropic force becomes $\boldsymbol{F} \approx -3\boldsymbol{R}/n$. The entropic spring stress is then $(3/n)\boldsymbol{RR} - 2\boldsymbol{I}$.

Let us consider the two halves of a bead–rod chain, each with $n/2$ beads, coming together as the chain relaxes. The friction factor associated with the motion of $n/2$ beads is just $n/2$ in the present units. Hence the collapse of the end-to-end length of the chain is roughly described by $(n/2)\dot{\boldsymbol{R}} = -(3/n)\boldsymbol{R}$, provided the chain is not too close to being fully stretched. Thus $\boldsymbol{R}$ decays exponentially at a rate $6/n^2$. The stress is $(3/n)\boldsymbol{RR} - 2\boldsymbol{I}$ according to the model, and so decays at a rate $12/n^2$. Given the crudeness of the model, we can hardly expect the coefficient 12 in $12/n^2$ to be correct, but at least the $O(1/n^2)$ scaling for the decay rate should be robust. In dimensional units this corresponds to an $O(k\hat{T}/\hat{\zeta}\hat{l}^2 \times 1/n^2)$ rate.

We have linearized the entropic spring force here, thereby requiring $|\boldsymbol{R}|/n$ be not too close to unity. The linearization should start to be approximately valid once the chain is less than about half of its fully stretched length. At this point $(3/n)\boldsymbol{RR}$ is $O(n)$. Hence in our stress relaxation simulations we expect an $O(n)$ value for σ_{11} decaying on an $O(1/n^2)$ time scale. Remember that the final equilibrium σ_{11} in our simulations

will be -1. The entropic spring formula $(3/n)\boldsymbol{RR}-2\boldsymbol{I}$ also gives an equilibrium value of -1 for σ_{11}, since $\langle \boldsymbol{RR}\rangle = (n/3)\boldsymbol{I}$ at equilibrium.

14. Rouse model

The entropic spring model gives the broad physical picture of the stress relaxation at long times. More sophisticated models yield more precise predictions. Fixman (1978*b*) has considered the relaxation of a variety of bead–spring and bead–rod chains, although not the freely jointed bead–rod chains we are considering. He focused primarily on the relaxation of chain modes, which are linear combinations of the link directors, which decay independently of one another. The longest wavelength modes determine the chain relaxation at long times. Fixman (1978*b*) found that the (appropriately non-dimensionalized) decay rate of the longest wavelength mode depended only on the number of links in the chain. It was independent of whether a bead–spring or bead–rod chain was being considered, and independent of other chain structural details. The decay rate for this particular mode can therefore be calculated from a particularly simple model, which is a freely jointed bead–spring chain, with Hookean springs (the Rouse model).

Since Hookean springs have no natural length, it is necessary to non-dimensionalize according to the equilibrium spring length, obtained by balancing the spring and thermal energy. For a spring constant $\hat{K}$, this length is $(3k\hat{T})^{1/2}/\hat{K}$, the factor 3 arising from the 3 degrees of freedom of a Hookean spring. We shall denote $(3k\hat{T})^{1/2}/\hat{K}$ by $\hat{l}$, a symbol earlier reserved (§2) for natural spring lengths. As mentioned earlier (§11) this choice of length scale implies that for Hookean springs there is no analogue of the dimensionless group K appearing in the bead–'Fraenkel spring' model.

The decay rate of the longest wavelength mode in the Rouse model with n links (Fixman 1978*b*) is $\lambda_1 = 12\sin^2(\pi/2(n+1))$, or $k\hat{T}/\hat{\zeta}\hat{l}^2 \times 12\sin^2(\pi/2(n+1))$ in dimensional units. For the Rouse model the long time stress decay rate is twice this rate. If $n \gg 1$, then this gives a rate $6\pi^2/n^2$ with an $O(1/n^3)$ correction.

In addition to the decay rates, the Rouse model also predicts amplitudes of each mode. Consider a chain initially stretched straight, with all link lengths equalling the equilibrium length, with say $\boldsymbol{D}_i = \boldsymbol{e}_1$. The amplitude of the longest wavelength mode is found by summing over the $\boldsymbol{D}_i$ with weightings $[2/(n+1)]^{1/2}\sin(i\pi/(n+1))$. The result for the straight configuration is $[2/(n+1)]^{1/2}\sin(\pi/(n+1))/\big(1-\cos(\pi/(n+1))\big)\,\boldsymbol{e}_1$. We can then show that the contribution to $\sigma_{11}+1$ from the longest wavelength is

$$\left(\frac{6\sin^2\big(\pi/(n+1)\big)}{(n+1)\big(1-\cos\big(\pi/(n+1)\big)\big)^2}-1\right)\exp(-2\lambda_1 t).$$

As $n\to\infty$, this formula is asymptotically $24n/\pi^2$, or $k\hat{T}\times 24n/\pi^2$ in dimensional units, and this agrees with the $O(n)$ stresses predicted by the entropic spring model.

Whilst the mode amplitude depends only on configuration, and not on the choice of model, the stress formula is specific to the Rouse chain. We see immediately how un-Rouse-like the bead–rod chain is at early times by comparing the initial stress in the two types of model. For the straight Rouse chain with unit link lengths we have $\boldsymbol{\sigma} = 3n\boldsymbol{e}_1\boldsymbol{e}_1 - (n+1)\boldsymbol{I}$. Contrast this with the vastly different stress formula for the exactly straight bead–rod chain $\boldsymbol{\sigma} = n(\frac{1}{3}n^2+n+\frac{5}{3})\boldsymbol{e}_1\boldsymbol{e}_1-(n+1)\boldsymbol{I}$ which was derived in §9.

We now summarize the results from this section. The Rouse model predicts an

exponential decay for stress at long times. For $n \to \infty$, the decay rate is $6\pi^2/n^2$, and the coefficient multiplying the exponential is $24n/\pi^2$.

15. Relaxation of polymer chains: long time scales

Now we consider how well the numerical results fit the Rouse model described in the previous section. It is sensible to consider data $(\sigma_{11}+1)/n$ plotted against t/n^2.

Ideally we wish to perform simulations for very long chains. There is however a computational problem. We saw in §12 that the initial decay involves $O(1/n^2)$ time scales. We must choose a time step smaller than this to resolve the rapid initial stress decay. Yet we expect that the full stress relaxation will involve $O(1/n^2)$ rates and therefore take $O(n^2)$ times. There are also $O(n)$ numerical operations to be performed at each time step. So overall the number of operations grows like n^5. Bear in mind also that we must perform many realizations to obtain good statistics. Clearly it is impractical to perform simulations for very large n, and we decided to simulate the full relaxation only as far as $n = 10$.

Fortunately we can anticipate that the time to reach equilibrium will be the multiple of n^2 with a fairly small numerical coefficient. This is because the Rouse model has a fairly large factor $6\pi^2$ appearing in the relaxation rate $6\pi^2/n^2$, and also because the trumbbell ($n = 2$) reached equilibrium by $t = 0.5$ (see figure 1). We simulated up to times $t = 0.25n^2$, which was more than sufficient to reach equilibrium.

We simulated bead–rod polymer chains with the number of links n taking the various values $n = 4$, $n = 6$, $n = 8$ and $n = 10$. We took a time step $0.01/n^2$, and 1000 realizations for each n. On the long time scales of interest, stress was averaged over several time steps in addition to averaging over the realizations, helping to reduce the statistical fluctuations.

In figure 4 we show $(\sigma_{11}+1)/n$ plotted against t/n^2 in a log-linear graph. Clearly $\sigma_{11}+1$ approaches an equilibrium value of zero as $t \to \infty$ as predicted in §9. Towards the bottom right-hand corner of the graph we find a random scatter starting to develop. This scatter arises from statistical fluctuations, which are magnified in this region of the graph by the log scale.

In the central region of the graph the points for each individual n lie along straight lines, meaning the stress has a Rouse-like simple exponential decay. The magnitude of the slopes seen on the graph does increase slowly with n. Best fit lines can be deduced by taking data for t/n^2 between 0.01 where the straight lines begin, and 0.06 where statistical fluctuations dominate. For instance for $n = 10$ we obtain $(\sigma_{11}+1)/n = 2.0\exp(-58.5\,t/n^2)$. For $n = 8$ the slope of the best fit line is 54.5, for $n = 6$ it is 52.4 and for $n = 4$ it falls to 43.4. Data for $n = 2$ have not been shown on figure 4, but are available from figure 1. For $n = 2$ a fit of the final stress decay to a decaying exponential in t/n^2 gives a slope 29.3.

The slopes for the different n fit the formula $70.2 - 129.7/n + 95.5/n^2$ with a correlation coefficient of 0.9977. A linear fit in $1/n$ gives instead $63.8 - 79.9/n$ with a correlation coefficient of magnitude 0.9891. These results suggest that the stress decay rate for a very long bead–rod chain will be between about $63/n^2$ and $71/n^2$, say roughly $70/n^2$. This decay rate exceeds the Rouse chain prediction of $6\pi^2/n^2 = 59.2/n^2$. It is unclear what accounts for the discrepancy in decay rates. Perhaps there is a small amount of a shorter wavelength (faster decay rate) mode contributing to the observed stress decay. However the data for each n fit a straight line well on figure 4, so the amplitude of any extra modes must be small. Another possible explanation for the observed 'faster than Rouse' decay in our data is that stress decay rates may exceed

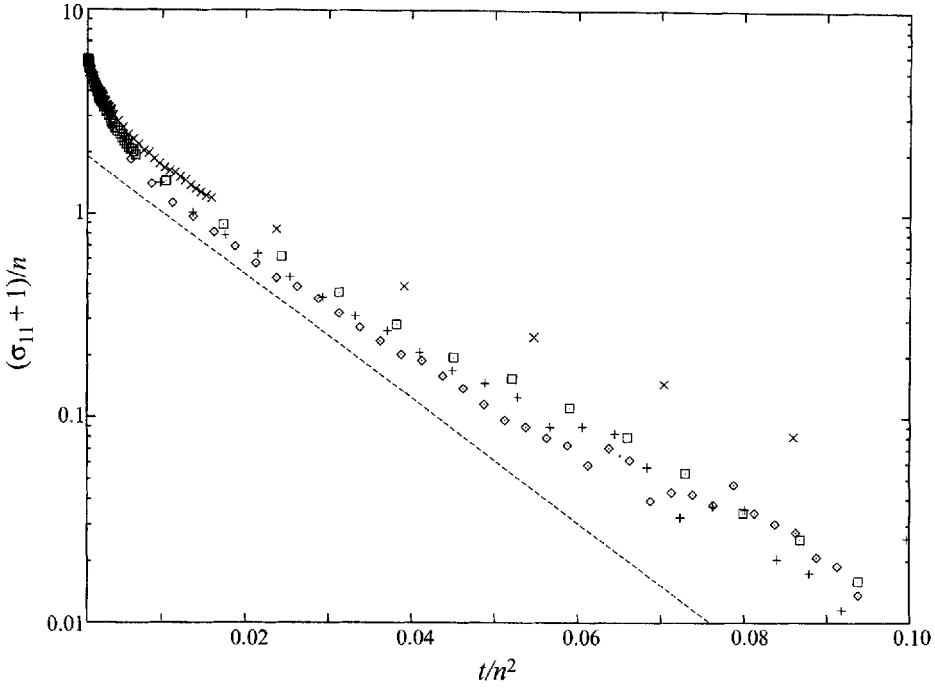

FIGURE 4. Relaxation of $(\sigma_{11}+1)/n$ on long time scales, with values $n = 10$ ◇, $n = 8$ +, $n = 6$ □ and $n = 4$ × and 1000 realizations in each case. Observe that the time axis is t/n^2, not simply t. For large t/n^2, $(\sigma_{11}+1)/n$ approaches 0, within statistical fluctuations, indicating the equilibrium value of σ_{11} is -1. In the central part of the graph the data lie along straight lines for each n, and the slope of these lines increases slowly with n. The change in slope with n is fit by the expression $70.2 - 129.7/n + 95.5/n^2$, which suggests the relaxation for $n \to \infty$ would follow the line $(\sigma_{11}+1)/n \approx 2.0\exp(-70.2\,t/n^2)$ (dashed).

twice the mode decay rates in certain bead–rod chains (Fixman 1978*b*). We comment however that the bead–rod chains in Fixman's study were not freely jointed.

Now we turn from a consideration of the slope of the lines in figure 4 (the decay rates), to an analysis of their intercepts. This involves extrapolating the long time stress decays back to the initial instant. The intercepts for the best fit lines take the values 2.0 ($n = 10$ and $n = 8$), 2.2 ($n = 6$) and 2.5 ($n = 4$ and $n = 2$). This appears to have a secular decrease with increasing n. However there is not a particularly good fit to these data in the form of a constant plus $O(1/n)$ and $O(1/n^2)$ corrections, so we are unable to extract reliably the $n \to \infty$ intercept from the present data.

Recall (§14) that the contribution of the longest wavelength mode to $(\sigma_{11}+1)/n$ in a straight Rouse chain with $n \to \infty$ is $24/\pi^2 = 2.43$. This is considerably larger than the intercept 2.0 for the bead–rod chain with $n = 10$. The trend of the numerical data suggests that for bead–rod chains with larger n, the discrepancy will be greater still.

The intercept obtained from extrapolating the long time stress decay of the bead–rod chain back to $t = 0$ is not directly related to the initial stress in the chain. Rather it will depend on how much of the mode amplitude for the longest wavelength mode remains when the Rouse-like simple exponential decay begins. The difference between the intercept for the bead–rod chain and the equivalent for the Rouse chain tells us therefore how effective the un-Rouse-like processes occurring in the bead–rod chain at early times have been at decreasing the amplitude of the longest wavelength mode.

The amplitude of the longest wavelength mode is closely related to the end-to-end

length of the chain. It would appear from our results that the bead–rod chain is more efficient at decreasing its end-to-end length than the equivalent Rouse chain. Physically we believe this is due to the differing distribution of tensions with respect to link location in the two types of chain. The tension equations defined in §10, along with the Kramers matrix of §9, suggest that the bead–rod tensions will generally peak in the chain centre whenever the link directors are roughly aligned. As a result of this, the beads feel an unbalanced force directed toward the centre of the chain. By comparing the unbalanced forces across each link, we find that the tensions cause the longitudinal projection of each link to decrease, giving considerable end-to-end shortening. For the straight Rouse chain on the other hand, the link tensions are initially uniform along the chain. In that case, the only beads which see an unbalanced tension force are those at either end of the Rouse chain, so only the outermost links will shorten initially.

The dashed line shown figure 4 satisfies $(\sigma_{11}+1)/n = 2.0\exp(-70.2\,t/n^2)$, and this should roughly fit the long time stress decay for large n. This line is obtained by taking the limiting slope 70.2 deduced from the numerical data at various n, with the intercept 2.0 of the best fit line for $n = 10$.

16. Relaxation of polymer chains: intermediate time scales

In the previous few sections we have established that there is an $O(n^3)$ stress on short $O(1/n^2)$ times and an $O(n)$ stress established on long $O(n^2)$ times. We wish now to investigate whether there is a simple stress decay law matching or joining these regimes. We search for a simple function which fits the data for times $n^2t \gg 1$ but $t/n^2 \ll 1$. Observe that $n^3(n^2t)^{-1/2} = n(t/n^2)^{-1/2} = n^2t^{-1/2}$, so that a $-\frac{1}{2}$ power law decay, with an $O(n^2)$ stress at $O(1)$ times, achieves the required matching. In dimensional units this corresponds to an $O(k\hat{T} \times n^2)$ stress per chain on $O(\hat{\zeta}\hat{l}^2/k\hat{T})$ times.

In figure 5 we have replotted the data from figure 3, this time on a log-log plot. The data do not show the full stress relaxation, only going up to a time $20/n^2$. For t greater than about $2/n^2$ the data do appear to lie along a straight line, with slope quite close to $-\frac{1}{2}$. Fitting the $n = 100$ data to a line with $-\frac{1}{2}$ slope over $2 \leqslant n^2t \leqslant 20$ gives $(\sigma_{11}+1)/\left(n\left(\frac{1}{3}n^2+n+\frac{2}{3}\right)\right) \approx 0.504\,(n^2t)^{-1/2}$ which can also be expressed as $(\sigma_{11}+1)/n^2 \approx 0.173\,t^{-1/2}$.

Now we consider whether this power law behaviour extends over the whole range $1/n^2 \ll t \ll n^2$, thereby giving the required matching between the short and long time regimes. To determine this, simulations are required up to times $0.01\,n^2$, since beyond $0.01\,n^2$ we know there is a simple exponential decay, not a power law decay. As in the previous section the amount of computation required becomes prohibitive for large n, and we have only considered values between $n = 4$ and $n = 12$.

The results of the simulations on intermediate time scales are shown in figure 6. The $-\frac{1}{2}$ power law line appears to be an asymptote for the data around the time $t \approx 0.1$, with the data points falling below the line for earlier or later times. The best fit for the asymptote is $(\sigma_{11}+1)/n^2 \approx 0.177\,t^{-1/2}$ as opposed to $0.173\,t^{-1/2}$ in figure 5. For larger n the data points stay close to the asymptotic line for longer time periods, with the $n = 12$ data laying close to the line for about one decade of the decay. Presumably yet higher n values would stay close to the line for several decades of the decay, and it would be instructive to perform more simulations with higher n. As stated above such simulations should be performed out to times $t \approx 0.01\,n^2$, since

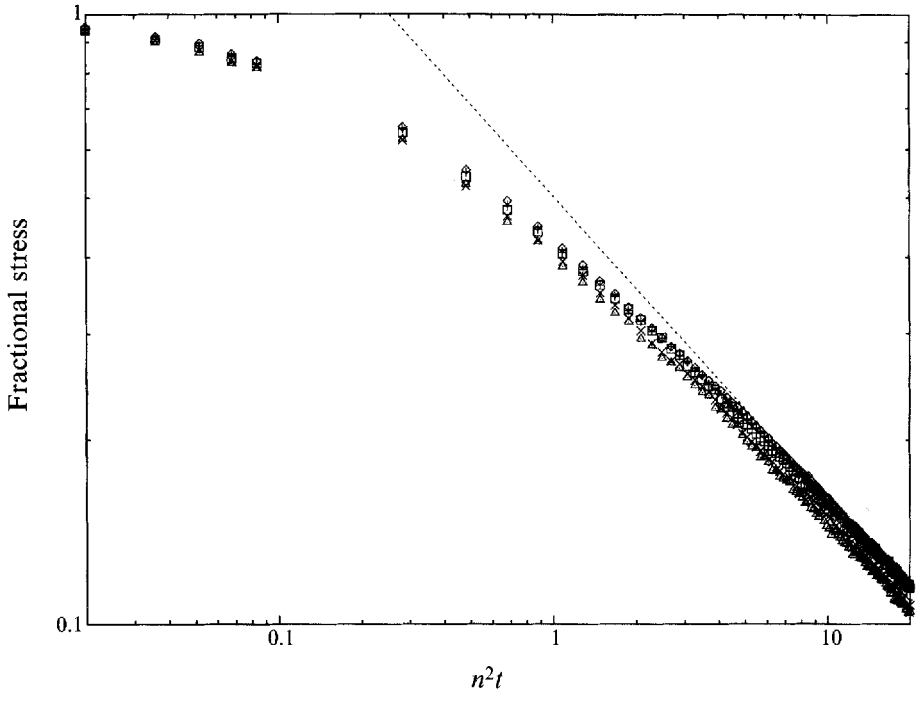

FIGURE 5. The short time scale data of figure 3 replotted on log-log axes. The number of links was $n = 100$ ⋄, $n = 50$ +, $n = 40$ ⊡, $n = 20$ × and $n = 16$ △, with 1000 realizations in each case. For n^2t greater than about 2, the data fall on a straight line with slope roughly $-\frac{1}{2}$. A fit for $n = 100$ on $2 \leqslant n^2t \leqslant 20$ gives $(\sigma_{11} + 1)/\left(n\left(\frac{1}{3}n^2 + n + \frac{2}{3}\right)\right) \approx 0.504\,(n^2t)^{-1/2}$, which can also be expressed as $(\sigma_{11} + 1)/n^2 \approx 0.173\,t^{-1/2}$ (dashed).

for later times the simple exponential decay of the previous section would replace the power law. It may be possible to circumvent the requirement for $O(n^5)$ numerical operations in the simulations (§15) by increasing the step size once the rapid short time stress decay is complete. Nonetheless the number of operations cannot be less than $O(n^3)$. It is clearly nonsensical to have Brownian displacements during a time step exceeding the lengths of the links, so δt must always be small compared to unity. Hence to reach $O(n^2)$ times we need $O(n^2)$ steps, with $O(n)$ operations per step. In the next section we present a theory which explains the $O(n^2t^{-1/2})$ stresses observed here.

17. Intermediate time scales: an explanation

We saw in §12 that when tensions limit the free sideways diffusion of the beads, the stress in the bead–rod chain starts to relax. In this section we extend this idea of tension-limited sideways bead motion to cover the intermediate time scale regime. Dimensional arguments will predict $O(n^2t^{-1/2})$ stresses on $O(1)$ time scales, as observed numerically in the previous section.

We start our analysis by considering an artificial physical system in which $n + 1$ beads are permitted to diffuse only in the 2,3 plane, subject to tensions held constant in time. We let z_i denote the displacement in the 2,3 plane of bead i and τ_i denote the ith tension. All the τ_i are assumed to be positive. The (deterministic) forces arising from the tensions are taken as $\tau_{i+1}(z_{i+1} - z_i) + \tau_i(z_{i-1} - z_i)$ and initially all the z_i are assumed to vanish. We also define the stress in the system (denoted σ_{11}) to be the

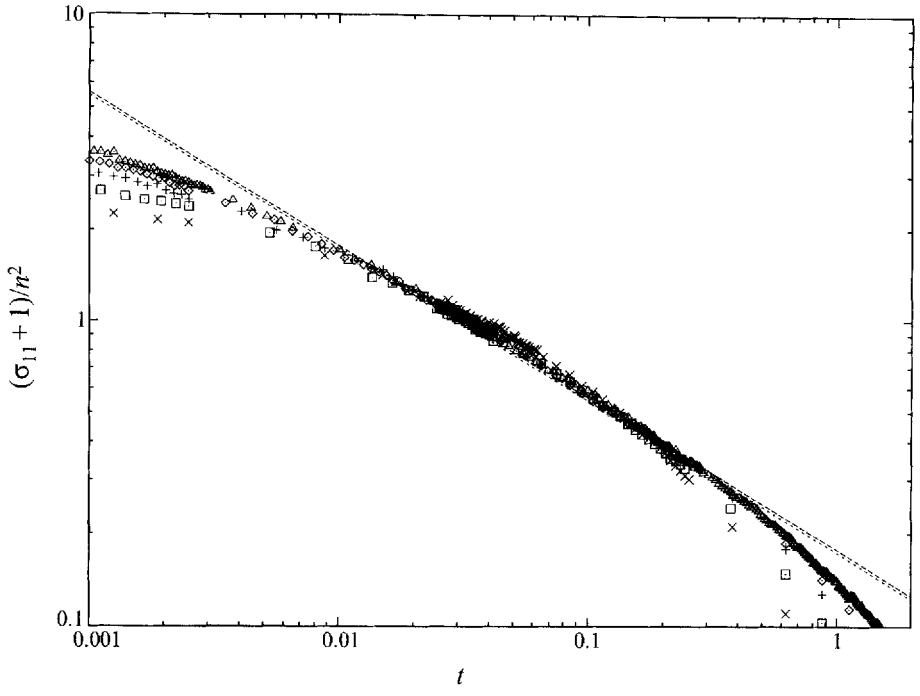

FIGURE 6. Relaxation of $(\sigma_{11}+1)/n^2$ on intermediate time scales plotted on log-log axes. The number of links was $n = 12$ △, $n = 10$ ◇, $n = 8$ +, $n = 6$ □ and $n = 4$ ×. A total of 1000 realizations were performed for each n. The data appear to asymptote to a line of slope $-\frac{1}{2}$. For larger n the data points stay close to the asymptotic line for longer time periods. The best fit line for $n = 12$ on $2/n^2 \leqslant t \leqslant 0.01\,n^2$ is $(\sigma_{11}+1)/n^2 \approx 0.177\,t^{-1/2}$ (long dashes). This lies very close to the best fit line from figure 5, which was deduced using data for $n = 100$ up to $t = 0.002$, and which was found to be $(\sigma_{11}+1)/n^2 \approx 0.173\,t^{-1/2}$ (short dashes).

sum of the τ_i. For convenience we shall refer to this model as the 'sideways motion' model. We emphasize that this artificial system is not intended to represent a relaxing polymer chain, since it only involves bead motion in two sideways directions, not in the longitudinal dimension. However, under certain conditions to be specified, the model can represent the sideways component of the bead motion in a bead–rod chain.

Hinch (1976*a*, *b*) has described a continuum theory for the sideways deviations of a flexible thread subject to Brownian motion and tension forces. This theory can be readily adapted to describe the discrete set of beads currently under consideration, and the equations obtained are essentially the same as for the continuum approach. The expected value of $z_i \cdot z_j$ evolves according to

$$\begin{aligned}\frac{\mathrm{d}\langle z_i \cdot z_j\rangle}{\mathrm{d}t} &- \tau_j\langle z_i \cdot z_{j-1}\rangle + (\tau_j + \tau_{j+1})\langle z_i \cdot z_j\rangle - \tau_{j+1}\langle z_i \cdot z_{j+1}\rangle \\ &- \tau_i\langle z_{i-1} \cdot z_j\rangle + (\tau_i + \tau_{i+1})\langle z_i \cdot z_j\rangle - \tau_{i+1}\langle z_{i+1} \cdot z_j\rangle \\ &= 4\delta_{ij}.\end{aligned}$$

Letting $\boldsymbol{Z}_i = z_i - z_{i-1}$ this can be manipulated to give

$$\begin{aligned}\frac{\mathrm{d}\langle \boldsymbol{Z}_i \cdot \boldsymbol{Z}_j\rangle}{\mathrm{d}t} &- \tau_{j-1}\langle \boldsymbol{Z}_i \cdot \boldsymbol{Z}_{j-1}\rangle + 2\tau_j\langle \boldsymbol{Z}_i \cdot \boldsymbol{Z}_j\rangle - \tau_{j+1}\langle \boldsymbol{Z}_i \cdot \boldsymbol{Z}_{j+1}\rangle \\ &- \tau_{i-1}\langle \boldsymbol{Z}_{i-1} \cdot \boldsymbol{Z}_j\rangle + 2\tau_i\langle \boldsymbol{Z}_i \cdot \boldsymbol{Z}_j\rangle - \tau_{i+1}\langle \boldsymbol{Z}_{i+1} \cdot \boldsymbol{Z}_j\rangle \\ &= 4(-\delta_{ij-1} + 2\delta_{ij} - \delta_{ij+1}).\end{aligned}$$

For $t \to \infty$ there is a steady solution $\langle \boldsymbol{Z}_i \cdot \boldsymbol{Z}_j \rangle = 2\delta_{ij}/\tau_i$ corresponding to a probability distribution $\exp\left(-\sum_{i=1}^{n} \frac{1}{2}\tau_i \boldsymbol{Z}_i \cdot \boldsymbol{Z}_i\right)$. The argument of this exponential represents the work which must be done against tension forces to separate each pair of beads i and $i-1$ by $\boldsymbol{Z}_i$. Thus the equilibrium probability distribution may be considered to be a Maxwell–Boltzmann distribution.

We estimate the time for the equilibrium probability distribution to be attained as follows. If the τ_i are uniform along the chain (with some value τ say), we can show that the Rouse modes for the $\langle \boldsymbol{Z}_i \cdot \boldsymbol{Z}_j \rangle$ evolve independently. The weighting of the kth mode approaches equilibrium at a rate $8\tau \sin^2(k\pi/2(n+1))$. Thus equilibrium is attained for each mode at a time $O(1/\tau \sin^2(k\pi/2(n+1)))$, or roughly $1/\tau$ for short wavelength modes, and $4n^2/\pi^2\tau$ for the longest wavelength mode.

Thus far we have been considering tensions τ_i which are constant in time. If we allow time-varying (but still deterministic) tensions $\tau_i(t)$ then the above equations for the evolution of $\langle \boldsymbol{z}_i \cdot \boldsymbol{z}_j \rangle$ and $\langle \boldsymbol{Z}_i \cdot \boldsymbol{Z}_j \rangle$ are still valid, but will have no steady solution. Nonetheless if the tensions are evolving slowly enough there may be a quasi-steady solution $\langle \boldsymbol{Z}_i \cdot \boldsymbol{Z}_j \rangle \approx 2\delta_{ij}/\tau_i(t)$ corresponding to a probability distribution $\exp\left(-\sum_{i=1}^{n} \frac{1}{2}\tau_i(t) \boldsymbol{Z}_i \cdot \boldsymbol{Z}_i\right)$.

Recall (§10, §12) that in the bead–rod model when the chain was nearly straight the expected value of the link tensions τ_i^{ra} satisfied

$$\langle \tau_i^{ra} \rangle = \tfrac{1}{2} A_{ij} \frac{\mathrm{d}}{\mathrm{d}t} \langle (\boldsymbol{z}_j - \boldsymbol{z}_{j-1}) \cdot (\boldsymbol{z}_j - \boldsymbol{z}_{j-1}) \rangle = \tfrac{1}{2} A_{ij} \frac{\mathrm{d}}{\mathrm{d}t} \langle \boldsymbol{Z}_j \cdot \boldsymbol{Z}_j \rangle,$$

with Kramers matrix A_{ij} defined in §9 and with summation over j.

We derived this equation earlier, but then simplified it further by assuming the beads were diffusing freely sideways. However in the present section we treat the case when the beads are not diffusing freely sideways, but rather their motion is limited by the tensions.

Suppose that we now choose the $\tau_i(t)$ in the above evolution equation for $\langle \boldsymbol{Z}_i \cdot \boldsymbol{Z}_j \rangle$ to equal these $\langle \tau_i^{ra} \rangle$ from the bead–rod model. Eliminating $\mathrm{d}\langle \boldsymbol{Z}_j \cdot \boldsymbol{Z}_j \rangle / \mathrm{d}t$ between the two sets of equations gives a tridiagonal system for the tensions

$$-(1 + \langle \boldsymbol{Z}_i \cdot \boldsymbol{Z}_{i-1} \rangle)\langle \tau_{i-1}^{ra} \rangle + 2(1 + \langle \boldsymbol{Z}_i \cdot \boldsymbol{Z}_i \rangle)\langle \tau_i^{ra} \rangle - (1 + \langle \boldsymbol{Z}_i \cdot \boldsymbol{Z}_{i+1} \rangle)\langle \tau_{i+1}^{ra} \rangle = 4.$$

We have a set of n^2 first-order differential equations plus this tridiagonal system to solve.

This 'sideways motion' model should approximately describe the transverse bead motion in the bead–rod case, provided $\boldsymbol{Z}_i$ retains magnitude smaller than 1. The stress in this model can be defined as

$$\boldsymbol{\sigma} = \sum_i \langle \tau_i^{ra} \rangle \boldsymbol{e}_1 \boldsymbol{e}_1 - (n+1)(\boldsymbol{I} - \boldsymbol{e}_1 \boldsymbol{e}_1) - \boldsymbol{e}_1 \boldsymbol{e}_1,$$

and this should also agree with the bead–rod stress at early times. Apart from the sum of the tensions, the term $-(n+1)(\boldsymbol{I} - \boldsymbol{e}_1 \boldsymbol{e}_1) - \boldsymbol{e}_1 \boldsymbol{e}_1$ in the above stress formula is included to agree with the 'random forcing' part of the bead–rod stress (cf. §9).

The agreement between the bead–rod model and the sideways motion model will probably be better for larger n. This is because the bead–rod τ_i^{ra} are weighted sums over all the $\mathrm{d}\boldsymbol{Z}_j \cdot \boldsymbol{Z}_j / \mathrm{d}t$ (cf. §10) and, when there are a large number of terms in the sum, the fluctuations in τ_i^{ra} about the expectation $\langle \tau_i^{ra} \rangle$ should be relatively small.

For present purposes we do not propose to supply detailed numerical solutions of the sideways motion model. It is sufficient to provide just an estimate to compare with the data from the bead–rod numerical simulations at intermediate time scales.

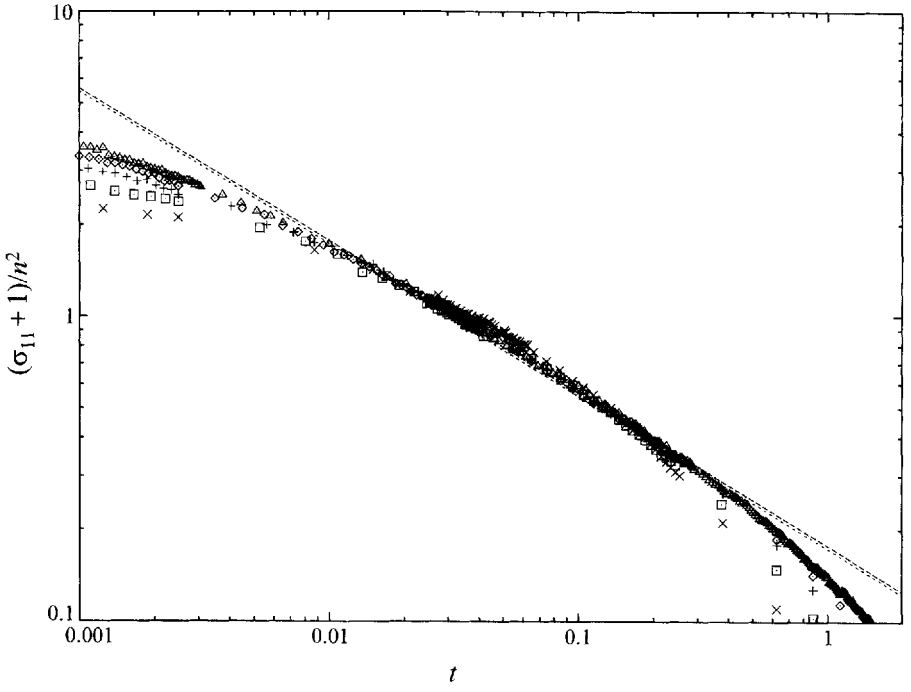

FIGURE 7. Growth of $\langle (z_{n/2} - z_{CM}) \cdot (z_{n/2} - z_{CM}) \rangle$ on intermediate time scales plotted on log-log axes. The number of links was $n = 12$ △, $n = 10$ ◇, $n = 8$ +, $n = 6$ ⊡and $n = 4$ ×. A total of 1000 realizations were performed for each n. The data asymptote to a line of slope $\frac{1}{2}$. This $t^{1/2}$ growth appears to be centred around $t \approx 0.8$, a contrast with the $t^{-1/2}$ stress decay in figure 6 which was found to be centred around $t \approx 0.1$. The best fit line for $n = 12$ over the range $100/n^2 \leqslant t \leqslant 0.01\,n^2$ is $\langle (z_{n/2} - z_{CM}) \cdot (z_{n/2} - z_{CM}) \rangle \approx 0.408\,t^{1/2}$ (long dashes). If the beads were to diffuse freely sideways then $\langle (z_{n/2} - z_{CM}) \cdot (z_{n/2} - z_{CM}) \rangle$ would equal $4t\left(1 - 1/(n+1)\right)$ or simply $4t$ for large n. This line is shown on the figure (short dashes).

Supposing then that a quasi-static solution exists for the sideways motion model we have $\tau_i = 2/\langle \boldsymbol{Z}_i \cdot \boldsymbol{Z}_i \rangle$. Equating this to $\langle \tau_i^{ra} \rangle$ gives

$$\frac{2}{\langle \boldsymbol{Z}_i \cdot \boldsymbol{Z}_i \rangle} = \tfrac{1}{2} A_{ij} \frac{\mathrm{d}}{\mathrm{d}t} \langle \boldsymbol{Z}_j \cdot \boldsymbol{Z}_j \rangle.$$

This is a set of n nonlinear first-order differential equations for the $\langle \boldsymbol{Z}_i \cdot \boldsymbol{Z}_i \rangle$. We can give order of magnitude estimates for the solutions. The A_{ij} are typically $O(n)$, except near the ends of the chain, so that the $\langle \boldsymbol{Z}_i \cdot \boldsymbol{Z}_i \rangle$ must be $O(t^{1/2}/n)$. The corresponding tensions τ_i are $O(nt^{-1/2})$. The stress σ_{11} is obtained essentially by summing the tensions and is thus $O(n^2 t^{-1/2})$, precisely as observed numerically in the simulations of the previous section. A continuum analogue of the present model exists and predicts a stress $0.19\,n^2 t^{-1/2}$ for the quasi-static regime, in fair agreement with the data of figure 6 which gave $0.177 n^2 t^{-1/2}$.

The above analysis gives us information about how rapidly adjacent beads separate in the transverse direction, but does not directly tell us how rapidly an individual bead moves. Indeed the relationship between $\langle \boldsymbol{Z}_i \cdot \boldsymbol{Z}_i \rangle$ and $\langle z_i \cdot z_i \rangle$ depends on the typical wavelength of the sideways bead displacements. If this wavelength is $O(n)$ then $\langle z_i \cdot z_i \rangle \approx n \langle \boldsymbol{Z}_i \cdot \boldsymbol{Z}_i \rangle \approx O(t^{1/2})$. Figure 7 shows some data in support of the proposed quasi-static transverse bead motion. We have plotted the time evolution of the mean

square sideways displacement of the central bead in the chain (with the centre of mass motion eliminated) $\langle (z_{n/2} - z_{CM}) \cdot (z_{n/2} - z_{CM}) \rangle$. Like the stress in figure 6, these data also asymptote to a line corresponding to the quasi-static regime. The best fit formula for the asymptote is $\langle (z_{n/2} - z_{CM}) \cdot (z_{n/2} - z_{CM}) \rangle \approx 0.408\, t^{1/2}$. Unlike the case of figure 6, where the asymptote is centred around $t \approx 0.1$, here the quasi-static asymptote is centred at $t \approx 0.8$.

The discrepancy in the time required to achieve the asymptote ($t \approx 0.1$ *vs.* $t \approx 0.8$) arises because the actual sideways motion of the beads is a little more complicated than the simple order of magnitude estimate suggests. The sideways bead positions are determined by summing over many modes, with the wavelengths of the modes ranging from $O(1)$ to $O(n)$. The short wavelength modes become quasi-static at $O(1/n^2)$ times, but the long wavelength modes only turn quasi-static much later. The tension may well be weighted toward short wavelength modes, whilst $\langle (z_{n/2} - z_{CM}) \cdot (z_{n/2} - z_{CM}) \rangle$ is weighted toward long wavelength modes. Hence the stress σ_{11} displays the quasi-static $n^2 t^{-1/2}$ decay some time before $\langle (z_{n/2} - z_{CM}) \cdot (z_{n/2} - z_{CM}) \rangle$ exhibits the quasi-static $t^{1/2}$ growth.

For steady tensions, uniform along the chain with value τ we have stated that the kth mode reaches equilibrium at time $O(1/\tau \sin^2(k\pi/2(n+1)))$. For unsteady tensions, we can expect quasi-static equilibrium when $t\tau(t) \sin^2(k\pi/2(n+1)) > O(1)$ where $\tau(t)$ is some typical average tension along the chain. Setting $\tau = nt^{-1/2}$ implies $t > O(1/n^2 \sin^4(k\pi/2(n+1)))$ for quasi-static equilibrium. For short wavelength modes this is simply $t > O(1/n^2)$, but long wavelength modes will not reach quasi-static equilibrium until $t = O(n^2)$.

The sideways motion model is only an accurate description of the bead–rod chain if $\boldsymbol{Z}_i \cdot \boldsymbol{Z}_i \ll 1$. According to the quasi-static estimates, this implies $t^{1/2}/n \ll 1$, or $t \ll n^2$. We have already seen that for $t \geqslant O(n^2)$ the relaxation is described by a simple Rouse-like decay.

We conclude that, for short wavelength modes, there can be a time interval in which both the bead–rod model will be approximated by the sideways motion model, and the sideways motion model will evolve quasi-statically. However for longer wavelength modes, the sideways motion model will cease to be an accurate description of the bead–rod chain, before the quasi-static regime is attained.

The simulations have been performed ignoring the effects of excluded volume. However excluded volume effects will have no influence in the intermediate time regime where beads move predominately sideways and the link directors are still essentially longitudinal. We can estimate the relative amounts of sideways and longitudinal motion via the following argument. The growth rate of the sideways link projections in the quasi-static regime is $\mathrm{d}(\langle \boldsymbol{Z}_i \cdot \boldsymbol{Z}_i \rangle)^{1/2}/\mathrm{d}t = O(t^{-3/4}/n^{1/2})$, while the links shorten longitudinally at rates roughly $\frac{1}{2}\,\mathrm{d}\langle \boldsymbol{Z}_i \cdot \boldsymbol{Z}_i \rangle/\mathrm{d}t = O(t^{-1/2}/n)$. The longitudinal rate begins to exceed the sideways rate at $O(n^2)$ times. Thus the onset of the simple Rouse-like decay at $t = O(n^2)$ corresponds to a change from a primarily sideways bead motion to one that is primarily longitudinal, as described in §13.

In summary, the stress evolution of the bead–rod chain on intermediate time scales $O(1/n^2) \leqslant t \leqslant O(n^2)$ is governed at least approximately by a quasi-static balance between link tensions and bead diffusion. This predicts that the mean-square sideways bead displacement will grow like $t^{1/2}$ (not like t as in free sideways diffusion), and the stress σ_{11} is $O(n^2 t^{-1/2})$ as observed in our data.

18. Conclusions

Computer simulations are a useful tool for investigating the influence of Brownian motion on polymer chain rheology. The bead–rod model for the chain is especially suited to numerical simulations, since it does not attempt to resolve very rapid (but rheologically uninteresting) processes, such as oscillations in the length of the individual links in the chain. This permits the use of a larger numerical time step, allowing the simulations to focus on the less rapid configurational changes of the entire chain, which have most bearing on polymer rheology.

Care must be exercised when performing the bead–rod simulations. A midpoint stepping scheme must be used to give the correct bead drifts, and additionally a pseudopotential must be added to account for the difference between the bead–rod statistics and bead–spring statistics, the latter being physically correct for real polymer chains. If the bead positions are to be described by Cartesian coordinates subject to constraints, then we must also ensure that random forces chosen by the simulations act only in certain directions determined by the constraints. When all these factors are taken into account, both the bead–rod model and the bead–spring model (with stiff Fraenkel springs) are found to exhibit the same stress relaxation, except for a very brief initial period associated with equilibration of the spring link lengths.

When calculating the stress contribution of a chain numerically, it is best to use a stress algorithm which eliminates any fluctuating terms of large magnitude known to have vanishing expectation value. This improves the quality of the statistics for the stress.

We have presented results showing the stress calculated as a function of time for a bead–rod chain, where the number of links, denoted n, ranges up to 100. The chain is initially stretched exactly straight, and then its configuration is allowed to relax due to Brownian motion. Physically this would correspond to stretching the chain by a strong flow and then switching off the flow allowing the chain to coil. Tensions appear in the links initially in order to maintain rod inextensibility as the beads diffuse freely sideways, and summing over these tensions gives the stress. The initial contribution to the bulk stress from each chain due to the tensions is $k\hat{T} \times n\left(\frac{1}{3}n^2 + n + \frac{2}{3}\right)$, roughly $k\hat{T} \times \frac{1}{3}n^3$ for large n. This contrasts with the entropic spring model, which would have an infinite stress for a completely aligned chain.

During the bead–rod chain relaxation, once the free sideways bead motion is arrested, the tensions maintaining rod inextensibility are also permitted to decrease. Initially an $O(k\hat{T}/\hat{\zeta}\hat{l}^2 \times n^2)$ relaxation rate for the stress is expected and indeed from the simulations the fastest relaxation rate is $k\hat{T}/\hat{\zeta}\hat{l}^2 \times 2.1\,n^2$ or in dimensionless units just $2.1\,n^2$. At long times, the stress has a Rouse-like simple exponential decay with an $O(k\hat{T}/\hat{\zeta}\hat{l}^2 \times 1/n^2)$ decay rate (for large n). However the actual rate for large n appears in dimensionless units to be $70/n^2$, compared with $6\pi^2/n^2$ in the Rouse model. At intermediate times there is evidence for a $t^{-1/2}$ power law decay in time, which would match the short and long time regimes. The stress is found to be $0.177\,k\hat{T} \times n^2 \times (k\hat{T}\hat{t}/\hat{\zeta}\hat{l}^2)^{-1/2}$ for times $O(\hat{\zeta}\hat{l}^2/k\hat{T} \times 1/n^2) \leqslant \hat{t} \leqslant O(\hat{\zeta}\hat{l}^2/k\hat{T} \times n^2)$, giving in dimensionless units an $0.177\,n^2t^{-1/2}$ stress for times between $O(1/n^2)$ and $O(n^2)$. This power law stress decay corresponds to a regime where tension forces quasi-statically balance the sideways diffusive forces on the beads in the chain.

Clearly during the relaxation there is a large relative change in dimensionless decay rates from $O(n^2)$ (early times) to $O(1/n^2)$ (late times), and this limits the size of n in the simulations. Numerical time steps must be chosen smaller than $O(1/n^2)$ so as to see the rapid initial stress decay, whilst the simulation must proceed to $O(n^2)$ times if

we wish to see the final stress decay. At present only $O(n)$ arithmetic operations are required at each time step, so overall the amount of computation grows like $O(n^5)$. Bear in mind however that these $O(n^5)$ operations must be performed for each of many realizations. In practice the full stress relaxation can only be simulated for fairly small n. Nonetheless it may be possible to reduce the number of time steps required by taking larger steps as the tensions decay, especially as we have now determined the power law behaviour by which this decay proceeds. Moreover it may be only worthwhile to simulate up to the point where the Rouse-like decay begins, since the chain behaviour is presumably well understood thereafter.

The simulations we have performed represent modest progress toward the goal of producing constitutive relations for polymeric solutions. Our aim has been to extract key features of chain physics which may have a bearing on a constitutive model. One feature we have discovered for instance is that for short and intermediate time scales the bead motion is predominately sideways. Moreover an initially free sideways bead motion (short times) gives way to a quasi-static regime (intermediate times). The 'sideways motion' model, formulated in this paper may well reward further study.

By no means have we exhausted the scope for performing numerical simulations with the bead–rod model. In future we hope to perform numerical simulations for a bead–rod chain in an applied flow field. A host of relevant questions arise. How rapidly does the chain reach equilibrium? What is the stress in the equilibrium state? What differences in chain behaviour do we see in extensional flow as opposed to shear flow?

Hydrodynamic interactions have been ignored in the stress relaxation results we have presented. Incorporating these would involve considerably more computational effort at each time step, both in choosing random forces acting only in allowed directions, and in calculating the tensions required to maintain inextensibility. For the early part of the relaxation, when the chain is nearly straight, the effect of hydrodynamic interactions can be estimated by considering slender body theory (Hinch 1976*b*). The most important slender body effect is that the friction of the straight chain is reduced by an $O(\log n)$ factor, leading to a more rapid relaxation. At long times hydrodynamic interactions would reduce the friction of the chain by an $O(n^{1/2})$ factor, meaning the long time decay rates would scale like $O(1/n^{3/2})$, instead of $O(1/n^2)$, giving Zimm rather than Rouse relaxation rates (de Gennes 1990).

P. Grassia is grateful to the University of Western Australia for financial support in the form of a Hackett Studentship. Computing facilities were provided by the SERC 'Computational Science Initiative' Grant GR/H57585, and an additional grant from the 'DTI LINK programme on Colloids'. P. Grassia also acknowledges partial support from CCE Contract CI*-CT91-0947 awarded by CONICYT, Chile.

Appendix

In §6 we introduced the pseudopotential forces needed to convert the statistics of a bead–rod chain to the physically correct statistics of a bead–spring chain. In this appendix we shall describe, for a chain of n links, how to calculate the pseudopotential forces on all the beads in $O(n)$ numerical operations. It is computationally important to be able to do this, since (without pseudopotential forces) there are $O(n)$ numerical operations per time step and we do not want the introduction of pseudopotentials to vastly increase the computational expense.

The key to efficient computation of pseudopotential forces is as follows. For each

bead i, at location $\boldsymbol{X}_i$, we must extract those terms from the pseudopotential which depend on $\boldsymbol{X}_i$. When we take gradients of the pseudopotential to obtain the forces, the ∇_i operators will only act on the $\boldsymbol{X}_i$ terms we have extracted, giving relatively simple expressions for the forces.

We recall the notation introduced in §2 in which $\boldsymbol{X}_i$ is the location of bead i, $0 \leqslant i \leqslant n$, and adjacent vectors are joined by $\boldsymbol{D}_i = \boldsymbol{X}_i - \boldsymbol{X}_{i-1}$, $1 \leqslant i \leqslant n$. We define the link length $l_i = (\boldsymbol{D}_i \cdot \boldsymbol{D}_i)^{1/2}$, and the unit vector directed along link i, $\boldsymbol{d}_i = \boldsymbol{D}_i/(\boldsymbol{D}_i \cdot \boldsymbol{D}_i)^{1/2}$, observing that $\boldsymbol{D}_i = l_i \boldsymbol{d}_i$. We impose the constraint that $l_i = 1$ for $1 \leqslant i \leqslant n$.

The pseudopotential (Fixman 1974; Hinch 1994) for the freely jointed bead–rod chain is $\log \sqrt{\det}$ where det is the determinant of an $n \times n$ tridiagonal matrix whose non-zero elements in the ith row are $-\boldsymbol{d}_i \cdot \boldsymbol{d}_{i-1}$, 2 and $-\boldsymbol{d}_i \cdot \boldsymbol{d}_{i+1}$.

We define $\det_{<i}$ to be the determinant of the submatrix formed by rows and columns 1 to $i-1$ of the $n \times n$ matrix. Similarly we define $\det_{>i}$ to be the determinant of the submatrix formed by taking rows and columns $i+1$ to n of the $n \times n$ matrix.

Note that $\det_{<1} = 1$ and $\det_{<2} = 2$, with remaining $\det_{<i}$ given by a recurrence relation (Fixman 1974)

$$\det_{<i+1} = 2 \det_{<i} - (\boldsymbol{d}_{i-1} \cdot \boldsymbol{d}_i)^2 \det_{<i-1}. \tag{A 1}$$

Similarly $\det_{>n} = 1$ and $\det_{>n-1} = 2$. The remaining $\det_{>i}$ for i ranging from $n-2$ down to 0 are given by the recurrence relation

$$\det_{>i} = 2 \det_{>i+1} - (\boldsymbol{d}_{i+1} \cdot \boldsymbol{d}_{i+2})^2 \det_{>i+2}. \tag{A 2}$$

Clearly, using these recurrence relations, the entire set of $\det_{<i}$ and $\det_{>i}$ can be obtained in $O(n)$ arithmetic operations. Note that $\det_{>0} = \det_{<n+1}$ and that these are just the determinant of the full $n \times n$ matrix, which we denote simply as det.

The recurrence relation (A1) above is useful for calculating the pseudopotential force on bead n, if we set $i = n$. Note that $\det_{<n-1}$ and $\det_{<n}$ are both independent of $\boldsymbol{X}_n$, as is $\boldsymbol{d}_{n-1}$. Also

$$\nabla_n \boldsymbol{d}_n = \nabla_n \frac{\boldsymbol{D}_n}{(\boldsymbol{D}_n \cdot \boldsymbol{D}_n)^{1/2}} = \nabla_n \frac{\boldsymbol{X}_n - \boldsymbol{X}_{n-1}}{[(\boldsymbol{X}_n - \boldsymbol{X}_{n-1}) \cdot (\boldsymbol{X}_{n-1} - \boldsymbol{X}_{n-1})]^{1/2}} = \frac{1}{l_n}(\boldsymbol{I} - \boldsymbol{d}_n \boldsymbol{d}_n),$$

which becomes simply $\boldsymbol{I} - \boldsymbol{d}_n \boldsymbol{d}_n$ when we impose the constraint $l_n = 1$.

The pseudopotential force on bead n, denoted by $\boldsymbol{F}_n^{ps}$, is $-\frac{1}{2}(\nabla_n \det)/\det$. Setting $i = n$ in recurrence relation (A1), operating on this with ∇_n and taking account of the comments in the above paragraph we deduce

$$\begin{aligned} \boldsymbol{F}_n^{ps} &= (\boldsymbol{d}_{n-1} \cdot \boldsymbol{d}_n)(\boldsymbol{I} - \boldsymbol{d}_n \boldsymbol{d}_n) \cdot \boldsymbol{d}_{n-1} \frac{\det_{<n-1}}{\det_{<n+1}} \\ &= (\boldsymbol{d}_{n-1} \cdot \boldsymbol{d}_n)(\boldsymbol{d}_{n-1} - \boldsymbol{d}_{n-1} \cdot \boldsymbol{d}_n \boldsymbol{d}_n) \frac{\det_{<n-1}}{\det_{<n+1}}. \end{aligned}$$

Similarly recurrence relation (A2) with $i = 0$ can be used to get the pseudopotential force on bead 0, denoted $\boldsymbol{F}_0^{ps}$. We use $\nabla_0 \boldsymbol{d}_1 = -(\boldsymbol{I} - \boldsymbol{d}_1 \boldsymbol{d}_1)$, and deduce

$$\boldsymbol{F}_0^{ps} = -(\boldsymbol{d}_1 \cdot \boldsymbol{d}_2)(\boldsymbol{d}_2 - \boldsymbol{d}_1 \cdot \boldsymbol{d}_2 \boldsymbol{d}_1) \frac{\det_{>2}}{\det_{>0}}.$$

However the relations (A1)–(A2) are of less use in determining the pseudopotential force for beads not at either end of the chain. It is more useful to consider instead

the relation

$$\begin{aligned}\det = {} & \left(4-(\boldsymbol{d}_i\cdot\boldsymbol{d}_{i+1})^2\right)\det_{<i}\det_{>i+1}\\ & -2\,(\boldsymbol{d}_{i+1}\cdot\boldsymbol{d}_{i+2})^2\det_{<i}\det_{>i+2}(1-\delta_{in-1})\\ & -2\,(\boldsymbol{d}_{i-1}\cdot\boldsymbol{d}_i)^2\det_{<i-1}\det_{>i+1}(1-\delta_{i1})\\ & +(\boldsymbol{d}_{i-1}\cdot\boldsymbol{d}_i)^2(\boldsymbol{d}_{i+1}\cdot\boldsymbol{d}_{i+2})^2\det_{<i-1}\det_{>i+2}(1-\delta_{i1})(1-\delta_{in-1}),\end{aligned}\tag{A 3}$$

an expression which applies for any bead i in the interior of the chain ($i = 1,\ldots,n-1$).

This is a very convenient expression because $\det_{<i-1}$, $\det_{<i}$, $\det_{>i+1}$ and $\det_{>i+2}$ are all independent of $\boldsymbol{X}_i$, so ∇_i acting upon them gives zero. Thus to calculate the pseudopotential force on bead i, $\boldsymbol{F}_i^{ps} = -\frac{1}{2}(\nabla_i \det)/\det$, we only need to consider ∇_i acting upon the remaining terms of (A3), $\boldsymbol{d}_{i-1}\cdot\boldsymbol{d}_i$, $\boldsymbol{d}_i\cdot\boldsymbol{d}_{i+1}$ and $\boldsymbol{d}_{i+1}\cdot\boldsymbol{d}_{i+2}$. Therefore $\boldsymbol{F}_i^{ps}$ can be obtained in a straightforward but tedious manner, by repeatedly using the results that

$$\nabla_i\boldsymbol{d}_i = \boldsymbol{I}-\boldsymbol{d}_i\boldsymbol{d}_i,\quad \nabla_i\boldsymbol{d}_{i+1} = -(\boldsymbol{I}-\boldsymbol{d}_{i+1}\boldsymbol{d}_{i+1}),\quad \nabla_i\boldsymbol{d}_{i-1} = \nabla_i\boldsymbol{d}_{i+2} = 0.$$

We shall omit here the actual formula for $\boldsymbol{F}_i^{ps}$ which contains about a dozen terms.

If $\det_{>0}$ to $\det_{>n}$ and $\det_{<1}$ to $\det_{<n+1}$ have already been found, then finding each $\nabla_i \det$ (and hence $\boldsymbol{F}_i^{ps}$) only involves $O(1)$ further operations. Thus there are $O(n)$ operations required to find the entire set $\boldsymbol{F}_1^{ps}$ through $\boldsymbol{F}_{n-1}^{ps}$ via the expressions in (A3).

REFERENCES

ABE, A., JERNIGAN, R. & FLORY, P. 1966 Conformational energies of the *n*-alkanes and the random configuration of higher homologs including polymethylene. *J Am. Chem. Soc.* **88**, 631–639.

BIRD, R., CURTISS, C., ARMSTRONG, R. & HASSAGER, O. 1987 *Dynamics of Polymeric Fluids.* John Wiley & Sons.

ERMAK, D. L. & MCCAMMON, J. A. 1978 Brownian Dynamics with hydrodynamic interactions. *J. Chem. Phys.* **69**, 1352–1359.

FIXMAN, M. 1974 Classical statistical mechanics of constraints: a theorem & applications to polymers. *Proc. Nat. Acad. Sci. USA* **74**, 3050–3053.

FIXMAN, M. 1978*a* Simulation of polymer dynamics. I. General theory. *J. Chem. Phys.* **69**, 1527–1537.

FIXMAN, M. 1978*b* Simulation of polymer dynamics. II. Relaxation rates and dynamic viscosity. *J. Chem. Phys.* **69**, 1539–1545.

FLORY, P. 1969 *Statistical Mechanics of Chain Molecules.* John Wiley & Sons.

DE GENNES, P. G. 1990 *Introduction to Polymer Dynamics.* Cambridge University Press.

GOTTLIEB, M. & BIRD, R. B. 1976 A molecular dynamics calculation to confirm the incorrectness of the random-walk distribution for describing the Kramers freely jointed bead–rod chain. *J. Chem. Phys.* **65**, 2467–2468.

GRASSIA, P. 1994 Computer simulations of polymer Brownian motion. PhD thesis, University of Cambridge.

GRASSIA, P., HINCH, E. J. & NITSCHE, L. C. 1995 Computer simulations of Brownian motion of complex systems. *J. Fluid Mech.* **282**, 373–403.

HASSAGER, O. 1974 Kinetic theory and rheology of bead–rod model for macromolecular solution. I. Equilibria & steady flow properties. *J. Chem. Phys.* **60**, 2111–2124.

HERZBERG, G. 1945 *Molecular Spectra & Molecular Structure. Vol II. Infrared & Raman Spectra of Polyatomic Molecules.* Van Nostrand.

HINCH, E. J. 1976*a* The distortion of a flexible inextensible thread in a shearing flow. *J. Fluid Mech.* **74**, 317–333.

HINCH, E. J. 1976*b* The deformation of a nearly straight thread in a shearing flow with weak Brownian motions. *J. Fluid Mech.* **75**, 765–775.

HINCH, E. J. 1977 Mechanical models of dilute polymer solutions in strong flows. *Phys. Fluids* **20**, S22–S30.

HINCH, E. J. 1994 Brownian motion with stiff bonds and rigid constraints. *J. Fluid Mech.* **271**, 219–234.

VAN KAMPEN, N. G. 1981 Statistical mechanics of trimers. *Appl. Sci. Res.* **37**, 67–75.

KAYE, G. & LABY, T. 1973 *Tables of Physical and Chemical Constants.* Longman.

KIRKWOOD, J. & RISEMAN, J. 1956 The statistical mechanical theory of irreversible processes in solutions of macromolecules. In *Rheology Theory and Applications* (ed. F. Eirich), Vol. 1, ch. 13, p. 495 Academic. Also in *John Gamble Kirkwood Collected Works: Macromolecules* (ed. P. Aeur), pp 32–56. 1967 Gordon & Breach.

KIRKWOOD, J. & SLATER, J. 1931 The van der Waals forces in gases. *Phys. Rev.* **37**, 682–697. Also in *John Gamble Kirkwood Collected Works: Dielectrics–Intermolecular forces–Optical Rotation* (ed. R. Cole), pp. 147–162, 1995 Gordon & Breach.

KLOEDEN, P. & PLATEN, E. 1980 *Numerical Solutions of Stochastic Differential Equations.* Springer.

KRAMERS, H. A. 1946 The behaviour of macromolecules in inhomogeneous flows. *J. Chem. Phys.* **14**, 415–424.

LIU, T. W. 1989 Flexible polymer chain dynamics and rheological properties in steady flows. *J. Chem. Phys.* **90**, 5826–5842.

ØSKENDAL, B. 1985 *Stochastic Differential Equations: An Introduction with Applications.* Springer.

PITZER, K. 1959 Inter & intramolecular forces & molecular polarizability. *Adv. Chem. Phys.* **2**, 59–83.

RALLISON, J. M. 1979 The role of rigidity constraints in the rheology of dilute polymer solutions. *J. Fluid Mech.* **93**, 251–279.

RALLISON, J. M. & HINCH, E. J. 1988 Do we understand the physics in the constitutive equation? *J. Non-Newtonian Fluid Mech.* **29**, 37–55.

REIF, F. 1965 *Fundamentals of Statistical and Thermal Physics.* McGraw Hill.

ROUSE, P. 1953 A theory of the linear viscoelastic properties of coiling polymers. *J. Chem. Phys.* **21**, 1272–1280.

WEAST, R. (ed.) 1971–72 *CRC Handbook of Chemistry & Physics.* The Chemical Rubber Co.

ZIMM, B. 1956 Dynamics of polymer molecules: viscoelasticity, flow birefringence & dielectric loss. *J. Chem. Phys.* **24**, 269–278.